Synthesis and Characterization Techniques of Nanocomposite Polymer Electrolytes Membranes: An Overview

Markandey Singh[1], Ubaid Ahmad Khan[2], Anshuman Srivastava[2], Nidhi Asthana[3,4*]

[1]Department of Applied Science, Buddha Group of Institution, GIDA, CL-1, Sector 7, Gorakhpur-273209
[2]Mechanical Engineering Department, SIET, Prayagraj, India.
[3]Department of Physics, Babasaheb Bhimrao Ambedkar University, Lucknow, U.P. India.
[4]Department of Physics, Graphic Era (Deemed to be University), Dehradun, Uttarakhand, India.

Volume 1, Issue 4, July 2024
Received:10 June, 2024; Accepted: 6 July, 2024
DOI: https://doi.org/10.63015/5N-2432.1.4

**Correspondence Author: asthananidhi27@gmail.com*

Abstract: The nanocomposite polymer electrolytes (NCPEs) are receiving special attention, especially within the realm of Solid-State Ionics by virtue of potential applications in innovative ionic devices (electrochemical devices) like Smart windows, sensors, high-powered batteries, fuel cells, and supercapacitors. etc. Using nanocomposite constituents, a versatile and robust approach has been developed to achieve novel nanocomposite polymer electrolytes (NCPEs) with tailored structural, thermal, mechanical, electrical, and electrochemical characteristics. This study describes the techniques used for the synthesis of inorganic fillers such as ceramic, ferrites nanoparticle, and nanocomposite polymer electrolyte films and their characterizations with emphasis on the sol-gel technique as it pertains to in this work. Different characterizing techniques related to current investigations like XRD, Optical Microscopy, SEM, IR(FTIR), DSC, CV and electrical characterization techniques like Wagner's polarization, impedance spectroscopy, dielectric spectroscopy and modulus spectroscopy have been briefly discussed to allow an amateur to understand the importance of these techniques in materials research in general.

Keywords: Nanocomposite Polymer Electrolytes, Electrochemical Devices, Impedance Spectroscopy, Modulus Spectroscopy.

1. Introduction: Materials science, organic chemistry, inorganic chemistry, polymer science, and electrochemistry are all included in the highly specialised multidisciplinary topic of polymer nanocomposite electrolyte science. This field has attracted the attention of both academics and industry professionals for the last three decades due to the bright applications of these electrolytes. The synthesis and characterization of polymer nanocomposite electrolyte involves various physio-chemical experimental techniques [1-3]. Synthesis techniques that affect the regulation of particle size distribution, dispersion, and interfacial interactions are essential to realising the unique features of polymer nanocomposite electrolytes. Because each system differs in physiochemistry, it is impossible to create a single, universal technique for generating polymer nanocomposites. Instead, synthesis techniques for nanocomposites are very different from those for ordinary micro scale-filled composites. To form, each polymer system could need a unique set of processing conditions, and different synthesis methods might generally provide non-equivalent outcomes. Keeping this fact in mind all the techniques used in the present investigation for development of nanocomposite polymer electrolytes have been briefly overviewed to enable a fresher to understand the basics of these techniques. To develop a material with desirable properties, it is essential to characterize it. Characterization of materials encompasses the delineation of all attributes pertaining to the composition, structure, and other relevant properties of a specific material

composition that are necessary for replicating a material with a desired characteristic. Within the framework of nanocomposite polymer electrolytes, it is essential to study interaction among components, their morphology, thermal behavior, electrochemical behavior, and ion conducting properties. Thus, all the techniques associated with these investigations have also been reviewed to make the presentation comprehensive. Because of its potential use in cutting-edge electrochemical devices such as efficient fuel cells, high-performance batteries, supercapacitors, sensors, and smart windows, nanocomposite polymer electrolyte materials (NCPEs) have drawn interest recently.

When it comes to thin-film electrolytes (NCPEs), there are several benefits over liquid electrolytes. These include reduced corrosion and superior thermal stability, lightweight with excellent mechanical properties, flexibility, ease of manufacturing and processing, and the ability to establish effective electrode-electrolyte contact. A polymer electrolyte based on polyethylene oxide (PEO) and utilising plasticizer, inorganic filler, and alkali salts has been thoroughly investigated. Anion/cation mobility has been demonstrated to occur in the amorphous phase, and its dispersion is facilitated by a multifaceted process involving PEO segmental mobility. To prevent crystallisation, the pure polymer structure must be altered, salt must be added, or regular packing must be inhibited by one or more plasticizers or fillers. Filler added to the PEO/(PEO+salt) matrix is expected to improve PEO's polar properties and increase its electrical conductivity. Filler could be in different places in this system. It can preferentially enter amorphous areas of the polymer and substitute itself on the polymer chain at crystalline or amorphous borders. Furthermore, Magnetic resonance imaging contrast agents, DNA separation, tissue engineering, hyperthermia and magnetic drug targeting have all demonstrated the value of nanoparticles. Because of their special electrical, magnetic, and optical properties, materials with nanoscale microstructures—also known as nanocrystalline materials or nano-composites—are currently seemly more and more significant in terms of technology. Composite polymer electrolytes, such as nano-composite polymer electrolytes (NCPEs), have undergone thorough investigation within the field of electrochemical applications, owing to their capability to improve ionic conductivity. Incorporating another component into these electrolytes, like inorganic/ceramic material, a ferroelectric substance is a common practice in composite polymer electrolytes (CPE). This augmentation aims to enhance the mechanical, electrical, and optical characteristics of the electrolytes. This multifunctional response of material may hold great promise for the development of better materials for electrical and mechanical devices, such as Seals, sensors, loudspeakers, dampers, and magneto-resistive damping. High magneto-electronic sensitivity is seen in polymer ferrite nano-composite films due to the strong magnetism of the filler components. These polymer magnets are widely employed in many different industries, such as audio equipment, home tools, and electronic and communications devices. Ferrites' characteristics render them an effective filler for the creating nano-composites intended for electrochemical uses, including PEM fuel cells and regulated medication distribution systems. We have explored how drug delivery systems can be designed to adjust their delivery rate in response to changes in the surrounding environment, which is one of two approaches. Specifically, our research has focused on understanding the transport properties and structure of nano-dispersed proton-conducting polymer composite electrolytes (NCPEs) under varying conditions. The soft chemical process (sol-gel method) was used to create the material at the nanoscale. SEM, optical microscopy, DSC, and X-ray diffraction (XRD) have all been used in morphological and structural studies of CPE. Impedance spectroscopy was utilized to assess the electrical conductivity of the solution.

2. Materials and Methodology: Polymeric nanocomposite electrolytes based on polyethylene oxide (PEO) (M.W. ~6×10^5, ACROS Organics) have garnered extensive

research attention. This is primarily attributed to their singular helical structure, which promotes rapid ion transport and facilitates ionic conduction [4-6]. PEO has an inverse solubility relationship in the vicinity of the water's boiling point, despite being fully soluble in both warm and cold water [7]. Thus, at 98°C, the resin becomes insoluble in water and precipitates. In solution, PEO gives a pH ranging from 6.5 to 7.5 and is completely soluble in certain organic solvents such as chlorinated hydrocarbons. Limited solubility exists in a wide variety of other organic solvents *e.g.* acetone, anisole, butanol, butyl acetate, ethanol, isopropanol etc. The degree of crystallinity is likely to vary during material processing such as shearing and tableting. Electrochemically, they are classified as non - ionic polymers. The decomposition products of PEO are carbon monoxide and carbon dioxide [8]. They have a bulk density of, 500 kg/m^3 and contain less than 3% of silicon dioxide and 1% of volatiles. PEOs are tough, crystalline polymers at room temperature, and their glass transition temperature decreases slightly with increasing molecular weight from -45 to -53 °C. They are nontoxic, nonirritant, and do not generate residue, sediment, or vaporous elements [9]. Nonetheless, the conductivity of the electrolyte based on PEO is restricted by high crystalline phase concentration. This phenomenon primarily arises from the fundamental necessity for conduction, wherein the motion of ions is intricately linked to the segmental motion of flexible amorphous polymer phases [10–12]. Despite PEO's widespread industrial use and significance, the ionic conduction mechanism is still unclear. These favorable properties, unresolved condition mechanism and broad applicability of this polymer ranging from drug delivery systems [13] to super capacitors and solid-state batteries prompted to consider PEO as the host matrix for formation of nanocomposite polymer electrolytes. With the mindset of developing proton conducting electrolytes among various alkali salts ammonium salt namely Ammonium thiocyanate (NH_4SCN, Rankem India) of AR grade was selected for synthesis of polymer electrolytes and nanocomposite polymer electrolytes [14, 15]. Preference to NH_4SCN was given owing to its following distinctive properties. It readily dissolves in water, alcohol, methanol, and acetone. It is possessing low dissociation energy and easily dissociated on the application of small DC potential. It also contains smaller cation size and bigger anionic size. It is easily melted at 149.5ºC temperature and PH ranging between 4.5 to 6.0. Among the varieties of solvent water was taken as solvent to prepare polymer electrolytes and nanocomposite polymer electrolytes. The most prevalent substance on Earth, water was chosen as a protic and polar solvent for the creation of electrolytes because of its advantageous formation film-forming qualities. According to survey of literature varieties of inorganic oxides have been tried to develop composite polymer electrolytes like NiO_x, TiO_2, SiO_2, Al_2O_3, $BaTiO_3$, $SrTiO_3$ etc. [16-26]. Among these dispersoids, SiO_2 was undertaken as dopant filler for the development of NCPE owing their most abundance on Earth surface and it's possessing acidic behavior of filler particles. Besides the new varieties of dispersoid, namely, ferrites, was chosen in present studies. Among the various inorganic/organic inert fillers, ferroelectric fillers (ferrites) can be used as filler particles due their unique properties. Within the class of inorganic fillers, ferrite is thought to be another strong candidate for the formation of NCPE due to its fascinating structural and electrical properties. Filler particles are drawn to ferrite's high dielectric constant below the Curie temperature. Additionally, it exhibits super paramagnetic behaviour, which opens new uses for polymer electrolytes in the biomedical, tissue engineering, and drug delivery fields. After the materials selection, the next stage of experimental investigation involves synthesis of nanoparticles followed by development of electrolytes.

2.1. Synthesis of Nano Dispersoids: Over the year's variety of techniques have involved for the development of nano fillers and electrolytes as outlined under Chemical

reaction technique, heat-assisted chemical reaction technique, sol-gel technique, chemical precipitation, hydrothermal technique, chemical vapor deposition, laser ablation technique, arc dis-arc technique, ball milling technique, solution combination method, and ultrasonic technique. Among these techniques sol gel technique is relatively low-cost simple technique and has been preferred for present investigations. In general, ceramic oxides can be produced using the sol-gel method, employing both ex-situ and in-situ approaches. In the current study, an ex-situ process has been selected for the development of ferrite filler nanoparticles. However, silica nano-dispersoids were synthesized using an in-situ process. The nano size ferrite powder was synthesized following wet chemistry route (sol-gel process). A variety of nitrates, such as $Al(NO_3)2{\cdot}6H_2O$, $Mg(NO_3)2{\cdot}6H_2O$, $Fe(NO_3)3{\cdot}9H_2O$, and $Zn(NO_3)2{\cdot}6H_2O$ (all in AR grade), have been employed as starting reagents to generate Al_2+, Mg_2+, Fe_3+, Zn^2+, and Fe^2+ ions in a liquid solution. In this process, Al, Zn, Mg, and Fe nitrates (Rankem India) were dissolved in a mixture of water and ethanol, followed by the gradual addition of tetraethoxysilane (TEOS) and mixing at room temperature for a duration of 50-60 hours, with the molar ratio of EtOH = 3: 1: 10 TEOS: H2O [27,28]. The solution's pH was maintained between two and three. At 40ºC, the sols were left to gel. Following jellification, it was dried for fifty hours at 150 degrees Celsius. The powdered gels were then heated in a Canthal high temperature furnace to 700ºC for three hours and 1000ºC for two hours. To create fine ferrite powder (such as Zn ferrite nano power, Mg-Zn ferrite, and Al-Zn ferrite), the dried material was crushed. Tetraethyl orthosilicate (TEOS, Aldrich) was utilized as the starting material, ethanol as the solvent, and ammonia solution as a catalyst to create ceramic filler (SiO_2). TEOS underwent a two-step hydrolysis process to generate nano fillers of SiO_2. Through the implementation of a two-step sol-gel method, nanosized ceramic filler (SiO_2) was created. The sol-gel solution formed was continuously agitated for a duration of ten hours while being mixed in a stoichiometric manner in PEO solution (PEO disintegrated in de-ionized (DI) water at 40°C). Afterwards, we add salt (NH_4SCN) to the PEO-SiO_2 solution in the calculated ratio. Finally, a polypropylene dish was filled with this gelatinous polymer solution. Additionally, NH_4SCN was mixed stoichiometrically to a solution of PEO and SiO_2 in DI water to synthesise the polymer electrolyte sheets. Ultimately, room temperature drying of the solution cast film produced free-standing CPE films.

2.2. Sol-Gel Technique: The so-called sol-gel process involves the addition of polymers or gellifying chemicals, the development of an accompanying network of polymeric or polymetallic species in situ during the drying phase, or both. The acronym "sol-gel" originates from the term "solution-gelling," denoting the fundamental concept of the process where a liquid phase containing dissolved precursors transforms into a solid state via series of chemical reactions, including polymerization [29–33]. The term "sol-gel," which is another name for "wet-chemical," describes a broad range of reaction techniques used in the manufacture of numerous distinct products using a diverse range of chemical precursors [34]. Kakihana states that there are basically three types of sol gel routes: (a) colloidal sol-gel route; (b) inorganic sol-gel routes and (c) organic sol-gel routes [35] and briefly outlined below.

2.2.1. Colloidal Sol-Gel Method: This method requires the dispersion of colloidal particles. By managing the steric or electrostatic transactions among the colloidal particles, the sol can be transformed into a gel [36–37]. The colloidal sol-gel method is known as a "physical" gel pathway due to the prevalence of real forces such as Van Der Waals forces, electrostatic forces, and Brownian motion in the inter particle interactions within these sols.

2.2.2. Inorganic Sol-Gel Method: There are essentially two methods for creating inorganic polymeric oxide gels: either using metal alkoxides dissolved in organic solutions or

using metal salts mixed in organic or aqueous solutions stabilised with chelating ligands. The strong electropositive nature of the metal cations dominates the chemistry in both situations.

2.2.3. Organic Sol-Gel Method: An organic polymeric network is formed in the third sol-gel pathway. There are two ways to go about doing this. The first is an "in-situ" polymerization method in which organic monomers are polymerized to create the gel network. When performed in with metal ions, it is expected that all metal ions will be uniformly distributed throughout the organic polymeric network. The term "polymerized complex method" refers to a procedure that combines "in-situ" polymerization with the creation of metal-chelate complexes. The alternative method, known as "polymer precursor method," involves forming a thick solution containing metal ions, polymers, and a suitable solvent. The procedure includes creating the initial solution, forming a gel, converting organic materials through pyrolysis, and producing an amorphous oxide with low-temperature heat treatment; followed by compaction and transformation into the desired oxide phase with high-temperature heat treatment. An adaptable strategy for producing nanocomposite materials that conduct protons involves incorporating inorganic substances into a polymer membrane through in situ synthesis using the sol-gel technique [38]. It allows for low-temperature synthesis at nano- to sub-micrometer sizes, and the membranes produced by this process are often homogenous. The procedure should ideally start at room temperature when a molecular precursor solution is infused in the polymer matrix. The aqueous solution within the membrane proceeds to interact with the inorganic molecules, leading to the hydrolysis of the penetrating inorganic precursor. Subsequently, the membranes undergo treatment with suitable reagents to complete the condensation reactions. Presently, common precursors employed in the formation of hybrid organic–inorganic composites include TMOS and TEOS. These precursors typically exhibit limited compatibility with biopolymers, posing a challenge when utilizing them. These precursors are poorly soluble in water, which makes the supplement of organic solvents necessary and the source of the constraints. Additionally, alcohol is produced during the sol-gel process, and these precursors must operate in conditions with extremely high or low pH.

The formation of silica nanocomposite materials can be shown by the following scheme:

Precursor + H_2O *Hydrolysis* → Silanols *Condensation* → Sol *Cross-linking* → Gel

The plan consists of three main phases [39-40]

(i) The hydrolysis of the alkoxide occurs following its combination with water.

(ii) Condensation of the siliconol hydrolysis products results in oligomers organised in the shape of sol particles.

(iii) The sol particles cross-linking, which causes a change into a gel state.

The following reaction provides a general illustration of hydrolysis:

$$Si(OR)_4 + nH_2O \rightarrow (HO^-)nSi(-OR)_{4-n}nHOR \quad \ldots\ldots\ldots(1)$$

Where R = hydrocarbon radical and $n \leq 4$.

An alkoxyl group is substituted with a hydroxyl group to produce a silanol group (Si-OH). A silanol group acts as the exclusive mediator of condensation, with two primary pathways identified by the general reactions that follow:

$$(RO-)_{4-n}Si(-OH)n + (HO-)_nSi(-OR)_{4-n} \rightarrow (OH)_{n-1}(RO-)_{4-n}Si-O - Si(-OR)_{4-n}(OH)_{n-1} + H_2O \ldots\ldots\ldots\ldots\ldots(2)$$

and

$$Si(-OR)_4 + (HO-)_nSi(-OR)_{4-n} \rightarrow (RO-)_3Si-O - Si(-OR)_{4-n}(OH)_{n-1} + HO - R \ldots\ldots\ldots(3)$$

The result in each case is a dimer consisting of a few silicon atoms connected by a siloxane link. Condensation reactions involving the dimer can result in the creation of a trimer,

tetramer, and further. However, the process ends there, leaving only oligomers, or oligosiloxanes, as the product. They are ordered as colloid particles with nanoscale dimensions (sol) in the bulk fluid. The resilience of the sol to the coagulation at almost neutral pH is influenced by the negative charge on the particle surface.

The linking of particles constitutes the third phase, where the sol-gel transition occurs. This is facilitated by the condensation reactions (2) and (3), which cross-link them; a catalyst is typically needed to accelerate this process. Processing is frequently started by adding acid or alkali to the solution because the coagulation's negative charge, which is pH-dependent, causes the sol stability.

2.3 Synthesis of Polymer Electrolyte/ Nanocomposite Polymer Electrolytes (NCPEs): Many methods have been developed throughout the years after the initial study on polymer electrolytes. The prominent over are, Solution cast technique, Sol-gel technique in liquid electrolyte medium, Polymerization in the presence of liquid electrolyte medium, Soaking of liquid (LML)/liquid electrolyte in polymer Electrolyte/Polymer matrix and Phase inversion method.

2.3.1. Solution Cast Technique: Many methods have been developed throughout the years after the initial study on polymer electrolytes. Solution cast method is the most common, easy to use and cheapest technique used for preparation of polymer electrolyte films. Comparative study for the synthesis of nanocomposite polymers i.e.
Sol-Gel Processing of Polymers book provides a comprehensive introduction to the sol-gel technique applied specifically to polymers. It covers fundamental principles, processing methods, and applications, including nanocomposite synthesis [41]. Sol-Gel Science: The Physics and Chemistry of Sol-Gel Processing book discusses the fundamental science behind sol-gel processes. It covers both inorganic and organic-inorganic hybrid materials, providing a solid foundation for understanding the sol-gel technique [42]. Sol-Gel Nanocomposites review article discusses the synthesis and properties of nanocomposites prepared using the sol-gel technique. It highlights the advantages of sol-gel processing in achieving nanoscale control over material properties [43]. In this method, stoichiometric proportions of the polymer and additive salt/acid are mixed separately in suitable selected solvent. The two solutions are subsequently mixed and stirred together for certain duration of time at elevated temperature to form homogeneous viscous solution. Third component filler particle are dispersed heterogeneously to achieve the composite polymer electrolyte and continuously stirred for 8-10 h. This solution is then cast on a Teflon/Polycarbonate mould to remove solvent by slow evaporation in air at room temperature. This solution cast film was first dried in a BOD incubator at a constant temperature of 30 °C to produce the solvent free-standing films of NCPEs. It was then dried in a vacuum. It is already widely known that the type of solvent used, how quickly the solvent is removed, and the presence of leftover solvent all have a substantial influence on the morphology of the resulting polymer electrolytes. In addition, present impurities (mostly water), atmospheric condition and thermal treatment history further complicated the situation. Thus, it is essential to overcome these problems so that all the complexes same type exhibits similar phase diagram and other related properties. Therefore, consistency is extremely important while using this technique for preparation of polymer complexes. However, in practice there are no universally acceptable common criteria. Although several other techniques have been adopted by various researchers, they have not gained popularity due to their inherent drawbacks. In conclusion, it is possible to produce polymer electrolyte films of the required thickness with consistent reproducibility by carefully choosing the solvents and managing the entire synthesis process. Considering this, the solution casting technique has been used in the present investigation (Figure-1).

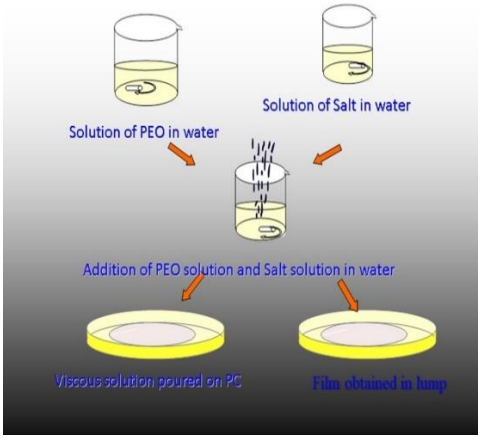

Figure-1 Synthesis of nanocomposite polymer electrolyte films

3. Characterization Techniques: As mentioned in previous section, it is necessary to characterize the material for structure, morphology, thermal behavior & mechanical, electrochemical, and electrical behavior to draw precise structure property correlation ship. This is pertinent to draw conclusion regarding applicability of materials in devices. Within the framework of ionic materials following techniques are usually employed to characteristics the material.

- ***Structure and Morphology:***

Optical microscopy, Infrared (IR) spectroscopy, Electron microscopy: SEM, TEM, and X-ray diffraction.

- ***Thermal Characterizations***

Thermo-gravimetric analysis, Differential thermal analysis and Differential scanning calorimetry, DMA/TMA, and Thermo-electrometry.

- ***Ion transport (Macroscopic)–Electrical Characterization Techniques***
- ***Transference and mobility measurement***

Wagner's polarization, Hittorf electrolysis, Coulometric analysis, combined ac/dc technique, Electro-gravimetric analysis, Transient ionic current measurement, and TCP and Electro-chemical potential measurement.

- ***Electrical Conductivity***

Complex impedance spectroscopy, two terminal dc technique with blocking electrode, four probe dc technique non-blocking electrode, two terminal ac technique or four terminal ac method, two terminal dc technique with non-blocking electrode and contact free induced torque method

- ***Diffusion Techniques***

Mass spectroscopy, Characteristic light absorption measurements, Spectro-photometric method, Electron spin resonance signal intensity measurements, radioactive tracer diffusion technique, Pulse field gradient NMR,

- ***Thermo-electric power, Electron microprobe technique,***
- ***Dielectric spectroscopy***
- ***Other conductivity related measurement***

(i)Viscosity measurement, (ii) pH measurement, (iii) Volume tracti-measurements-psychometric method (iv) Swelling and swelling kinetics

- ***Ion transport (microscopic)***

NMR line width and relaxation time, Quasi-elastic neutron scattering, Diffused x-ray and neutron scattering, Microwave and radio frequency relaxation spectroscopy, Raman scattering, Brillion scattering, Though, all these techniques have been described in standard texts, review papers and reporting of various workers, the techniques employed in the present investigation for characterization of nanocomposites polymer electrolytes would now be briefly described for coherence of presentation. A comparative study for characterization technique is cited below: Advanced Characterization Techniques for Nanocomposites review article provides an overview of advanced characterization techniques such as TEM, SEM, AFM, XRD, and spectroscopic methods applied to nanocomposites. It discusses recent advancements and their applications in understanding nanocomposite structures and properties [44]. Characterization Techniques for Polymer Nanocomposites: A Review discusses a wide range of characterization techniques used for polymer nanocomposites. It includes microscopy, spectroscopy, thermal analysis, mechanical testing, and surface analysis techniques, providing insights into their applications and advancements [45].

3.1. Structural Characterization: Structural characterization is crucial for understanding the formation of nanocomposite polymer electrolytes. In structural characterization, one can study physical/chemical structure and variety of concept describing the arrangement of building blocks of materials. Therefore, structural investigation constitutes on essential component of nanocomposite material research. As indicated earlier different scattering, spectroscopic, scanning and transmitting tools for structural characterization of materials have been developed over the decades. The morphological studies are yet other factor for the routine investigations of nanocomposite polymer electrolytes to obtain important information regarding association of structural units within nanosized structures. The techniques used for these investigations in present work would now be overviewed.

3.1.1. X-Ray Diffraction (XRD): A very efficient and widely available method for figuring out the atomic arrangement in materials is X-ray diffraction (XRD). Because of this, it is a flexible and often used instrument in solid-state physics to study the complex structures of matter. For the structural characterisation of materials in all forms, from powder, bulk, and films to single crystals, X-ray diffraction has proven to be an effective approach [46]. Besides this technique can be used in stress measurement study of phase equilibrium, determination of particle sizes and its orientations in crystal or ensembles of orientation in polycrystalline aggregate [47]. In case of polymers, polymer electrolytes and polymer nanocomposite electrolytes it has been used as routine investigation technique for elucidation of structure [48, 49]. Polymer nanocomposite electrolytes contain complex nano/micro heterogeneity scattering center with variable amount of crystalline and amorphous phases. Since the inorganic phases in nanocomposite electrolytes produced by the thermal breakdown of molecules typically have a crystalline form, wide angle X-ray powder diffraction is a straightforward method for identifying them. Such polymer-embedded nano-crystals have a broad diffraction pattern due to the small size of their crystalline domains (less than 50 nm). Furthermore, peaks in a nanocomposite sample often have modest intensities since the amount of inorganic phase in the sample is typically low. The majority of nanocomposite diffractograms have a low signal/noise ratio and only those signals that correspond to the most abundant crystallographic planes can be recognised. Only by utilising X-ray sources with sufficient anti-cathode materials and a modest angular movement of the detector can good quality diffraction data be obtained. Since nanoparticles are often single crystals, the distribution of peak intensities may also provide information about the shape of the particles, and the broadening of diffraction peaks permits an approximative assessment of crystallite size using Scherer's formula. Scherer's formula can be applied to determine the crystallite size from a diffraction pattern.

$$L = \frac{0.9\lambda}{\beta \cos\theta} \dots\dots\dots\dots (4)$$

Where L= the thickness of crystalline involved in diffraction of x-ray

λ= wavelength of X-ray

β= full width at half maxima of intensity and known as angular broadening and expressed in radians

θ= angle at maximum intensity for concerned peak

The main components of a typical XRD system are the X-ray source and detector. They are positioned around a circle known as the focusing circle, with the specimen positioned in its centre. An evacuated x-ray tube's metal target anode is the target of a high-voltage electron beam directed towards the source of x-rays. The x-ray protons of a given energy can be calculated by the detector for each angle 2θ, which is a proportionate reflection of the peak intensity. The relationship between the diffraction angle, atomic separation (d), and wavelength of the impinging X-ray beam is described by the Bragg equation (figure-2a).

$$2d \sin\theta = n\lambda \ldots\ldots\ldots (5)$$

Here, "n" represents an integer denoting the order of the diffraction peak.

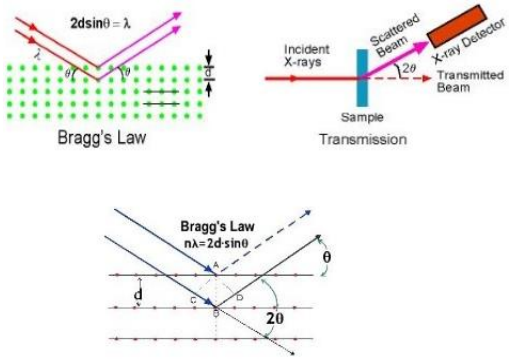

Figure 2(a). Bragg's diffraction of X-ray satisfying the interplanar distance (b) in crystalline materials [50]

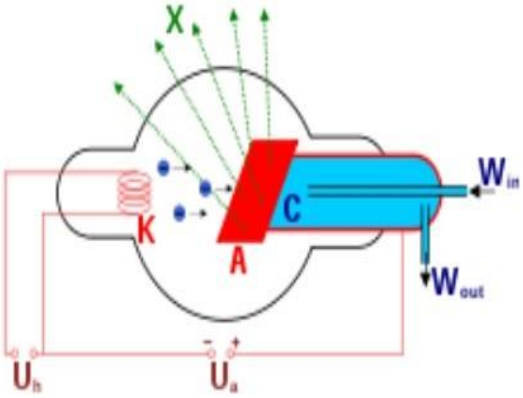

Figure 2(b). Diagram of water-cooled X-ray tube [51]

When using powder XRD, the sample is often made up of tiny grains of the single-crystalline substance that is being examined. This method is also frequently used to investigate polycrystalline solids (both bulk and thin film materials) as well as particles in liquid suspensions. This XRD technique was used in the current study to investigate the following parameters: Determining the configuration of crystalline substances involves assessing properties such as crystallographic axes, dimensions, and morphology of the fundamental unit, as well as the spatial arrangement of atoms within said unit; discerning the disparities between crystalline entities and disordered materials; and quantifying deformation and minute grain dimensions.

Using these parameters inferences would be drawn for complexation behavior of components present in nanocomposite electrolytes. The shift in peak intensity is due to change in interplanar spacing at diffraction angle (2θ) which gives information of complexation behavior and the variation in d values for diffraction pattern provide some information regarding the change in crystalline structure of samples. To distinguish the impact of broadening caused by crystallite size from that caused by strain on the Full Width at Half Maximum (FWHM) of the XRD profile, researchers use the Williamson-Hall plot method [52]. This method involves calculating the crystallite size using a relationship derived from the Sinθ vs. β Cosθ plot

$$\beta \cos\theta = \frac{C\lambda}{L} + 2\varepsilon \sin\theta \ldots\ldots\ldots (6)$$

where β =FWHM (full width at half maxima of intensity)

L= the grain size, C= the correction factor, ε = the strain λ= the wavelength of X-ray.

3.1.2. Optical Microscopy (OM): A microscope (figure-3) is a device utilized for observing tiny objects. Microscopy is the discipline dedicated to the examination of diminutive entities using such a tool. As the original and most widely used form, the optical microscope is well-known in this domain. This optical device has one or more lenses that, when an object is put in their focal plane, produce a magnified image of that thing. Using the optical theory of lenses, optical microscopes enlarge images that are produced when a wave passes through or is reflected off a material. A typical magnification of a light microscope, assuming visible range light, ranges up to 1500x, with a theoretical resolution limit of around 0.2 micrometres or 200 nanometres [53-54].

A specific type of micro-projection called photomicrography uses a detector to record

images of microscopic specimens that have been magnified by a microscope.

Figure 3. A Typical Optical Microscope [55]

The silver halide emulsion on glass or film served as the main photomicrography media for much of the 20th century. Since nearly the dawn of photography, these materials have faithfully reproduced countless images taken with an optical microscope, which has been of great assistance to the scientific community. Photomicrography is a phrase that can be used interchangeably with microphotography, which is the usual term for the technique of creating miniature images of huge items, including microfilms of books and documents. More specifically, the characteristics of the imaging device are important in defining the resolution that is obtained and the dynamics of the specimen visualisation [56].

3.1.3. Scanning Electron Microscope (SEM): An image of a specimen that has been electronically enlarged for close examination is produced by an electron microscope. The specimen is illuminated and a magnified image of it is produced by the electron beam used by the electron microscope (EM). In comparison to an optical microscope driven by light, the microscope has a higher resolving power (magnification) because it employs electrons with wavelengths that are around 100,000 times shorter than visible light (photons). Light microscopes are limited to magnifications of 1000x, but this one can reach up to 3,000,000x. A scanning electron microscope (SEM) produces various signals at the surface of solid objects by focusing a high-energy electron beam. The ray diagram of a typical scanning electron microscope is shown in the figure. SEM signals, generated by electron-sample interactions, provide information about the sample's materials, including their orientation, crystalline structure, chemical composition, and external morphology (texture). Most applications entail the collection of data across a specified portion of the sample's surface to generate a 2D image illustrating the spatial variations in these characteristics. Traditional SEM techniques are capable of investigating regions with widths ranging from approximately 1 cm to 5 microns in a scanning mode (with magnification levels from 20X to around 30,000X and spatial resolution of 50 to 100 nm). Also, the SEM can analyse points on the sample for purposes such as determining chemical compositions, crystalline structure, and crystalline orientation in a semi-quantitative or qualitative fashion. The Electron Probe Micro Analyzer (EPMA) and the SEM share many functional similarities, as well as a significant amount of capability overlap. The range of signals generated by electron-sample interactions includes Heat, secondary electrons (which create SEM images), backscattered electrons (BSE), diffracted backscattered electrons (EBSD), and photons (including distinctive X-rays used for elemental analysis). Secondary electrons and backscattered electrons are two of these radiation types that are frequently utilised to image samples. Backscattered electrons are particularly helpful for presenting morphology and topography on materials, while they also emphasise compositional contrasts in multiphase samples or for fast phase discrimination [57–58].

The SEM (depicted in Figure-4) facilitates precise measurement of exceedingly minute features and objects, with the capability to discern sizes as small as 50 nm.

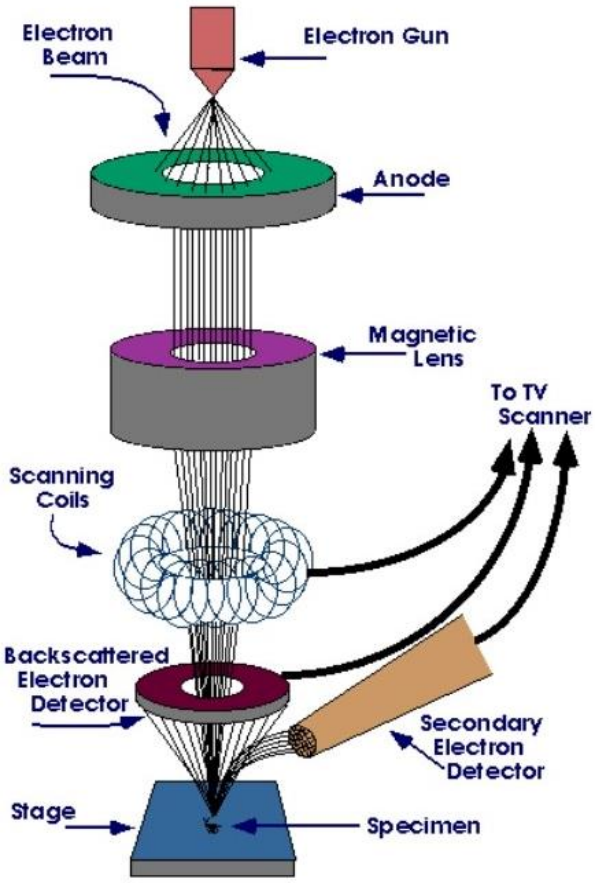

Figure 4. Ray diagram of scanning electron microscope (SEM) [59]

3.1.4. Infrared Spectroscopy: Finding the source of a pollution issue often requires first identifying an unknown material's chemical composition. The identification method might be especially difficult if the contaminant is organic in nature because there are thousands of different chemical components. Many contaminants are mixtures of two or more substances, making it more challenging to identify unknowns. Therefore, spectroscopic techniques like IR, NMR, and UV Raman Spectroscopy etc. have become many popular and most convenient probes for determination of local structure. Fourier Transform Infrared spectroscopy (FTIR) is a significant method among these spectroscopic approaches that is highly beneficial for the characterisation of organic materials. The presence of chemical structures can be inferred from the FTIR spectra [60]. It is a simple method of determining whether a molecule contains a particular functional group. Additionally, the distinct set of absorption bands can be used to identify specific contaminants or validate the identity of a pure molecule. An additional method to IR spectroscopy is Raman spectroscopy [61]. The principle behind Fourier Transform Infrared (FTIR) Spectroscopy is that nearly all molecules absorb infrared radiation. Monatomic molecules (such as He, Ne, Ar, etc.) and homopolar diatomic molecules (like H_2, N_2, O_2, etc.) are the sole types that do not absorb infrared light. Only those wavelengths of infrared light that alter a molecule's dipolar moment do molecules absorb it. The dipolar moment of a molecule is created by the variations in charges in the electronic fields of its atoms. Infrared photons can interact with molecules that have a dipolar moment, exciting them to higher vibrational states. Due to the equal electronic fields of all its atoms, homopolar diatomic molecules lack a dipolar moment. Since monatomic molecules only contain one atom, they do not have a dipolar moment. Therefore, infrared light is not absorbed by homopolar, diatomic, or monatomic molecules. Nevertheless, nearly every other molecule absorbs infrared light. Infrared spectroscopy primarily involves measuring the intensity of the infrared light spectrum that remains after passing through a sample, achieved by dispersing it using a Michelson interferometer. In FTIR spectroscopy, multiplexing allows for the simultaneous monitoring of all optical frequencies emitted by the source over a period. The electromagnetic spectrum's infrared region is typically segmented into three distinct areas: near-infrared, mid-infrared, and far-infrared, categorized based on their closeness to the visible light spectrum. The microwave region is adjace't to the low-energy far-infrared (400–10 cm−1; 1000–30 μm), which is suitable for rotational spectroscopy. Mid-infrared, roughly spanning 4000–400 cm−1 (30–2.5 μm), is where fundamental vibrations and their rotational-vibrational structures are studied. Near-infrared, with energies around 14000–4000 cm−1 (2.5–0.8 μm), can excite overtone or

harmonic vibrations. It is crucial to remember that these subregions' labels and categorization are purely traditional. They are not based on

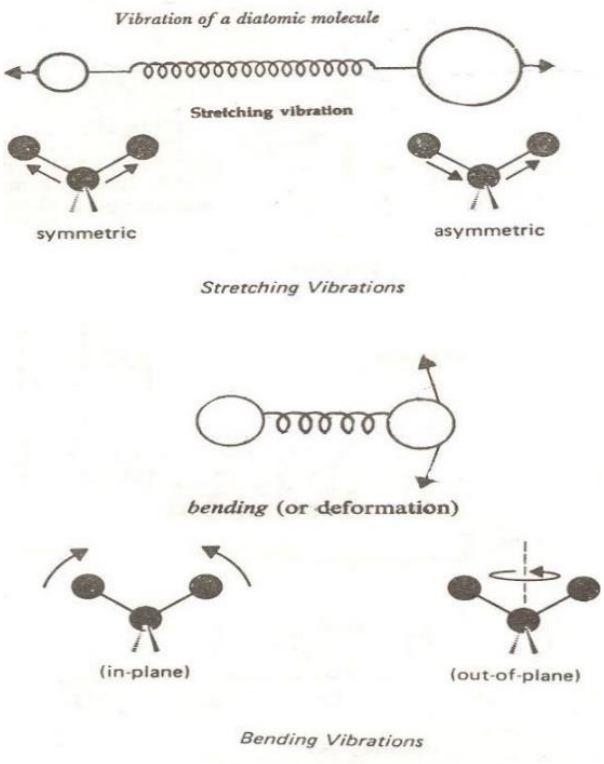

Figure 5(a). Vibration modes of molecules [62]

chemical or electromagnetic properties, nor are they well characterised. Molecules may perform stretching and bending of following type and as illustrated in figure -5(a).

The characteristics of stretching vibrations, including symmetric and asymmetric stretching vibrations, as well as bending vibrations such as Scissoring, Rocking, Wagging, and Twisting, can be observed in the absorption versus frequency profiles of infrared light passing through a sample. This serves as a unique fingerprint of the molecular structure, facilitating the identification of different compounds. To identify chemical bonds and groups in a complex molecule, molecular vibrations are detected and measured to retrieve information about structure and interaction. The compositional modification due to mass transport, heat, irradiation effect can also be detected by monitoring IR spectra [63-64]. Fraction of free ion and ion pair in polymer electrolyte can also be evaluated using IR spectra [65]. An infrared spectrum is typically analyzed in two distinct regions, namely:

(a) Finger print region 1300-650 cm^{-1}: The reason this region has its name is because no single compound absorbs in this fashion. Since both stretching and bending modes can result in absorption in the 1300–909 cm-1 area of the IR spectra, the intermediate section of the spectrum is typically complicated. Due to their nearly identical energies, single bonds are typically responsible for the formation of absorption bands in the finger print region. The absorption bands are thus composites of strong interaction which occurs between neighboring bonds and depends upon overall skeleton structure of molecule.

(b) Functional group region 4000-1300 cm^{-1} : Certain regions of the infrared spectrum correspond to characteristic stretching frequencies of significant functional groups. Infrared spectra of substances are also affected by the physical state, electronic environments, interaction that takes place between molecules, and lattice vibrations [66-68]. Therefore factors, like hydrogen bonding, coupling of oscillation and Fermi resonance electronic environment in immensely affect the position of absorption line. Table 2.1 broadly shows correlation bands to identify structure of the substance. Figure-5(b) shows basic diagram of a double beam infrared spectrometer normally used in IR studie

An infrared laser beam can be used to measure a sample's infrared spectrum. By examining the transmitted light, the quantity of energy consumed at each wavelength is calculated. This can be done with a device that measures all wavelengths simultaneously using the Fourier transform or with a monochromatic beam whose wavelength Variations over Time. A transmittance or absorbance spectrum that shows the infrared wavelengths absorbed by the material is the result. Understanding the sample's molecular structure is possible through analysis of these absorption properties.

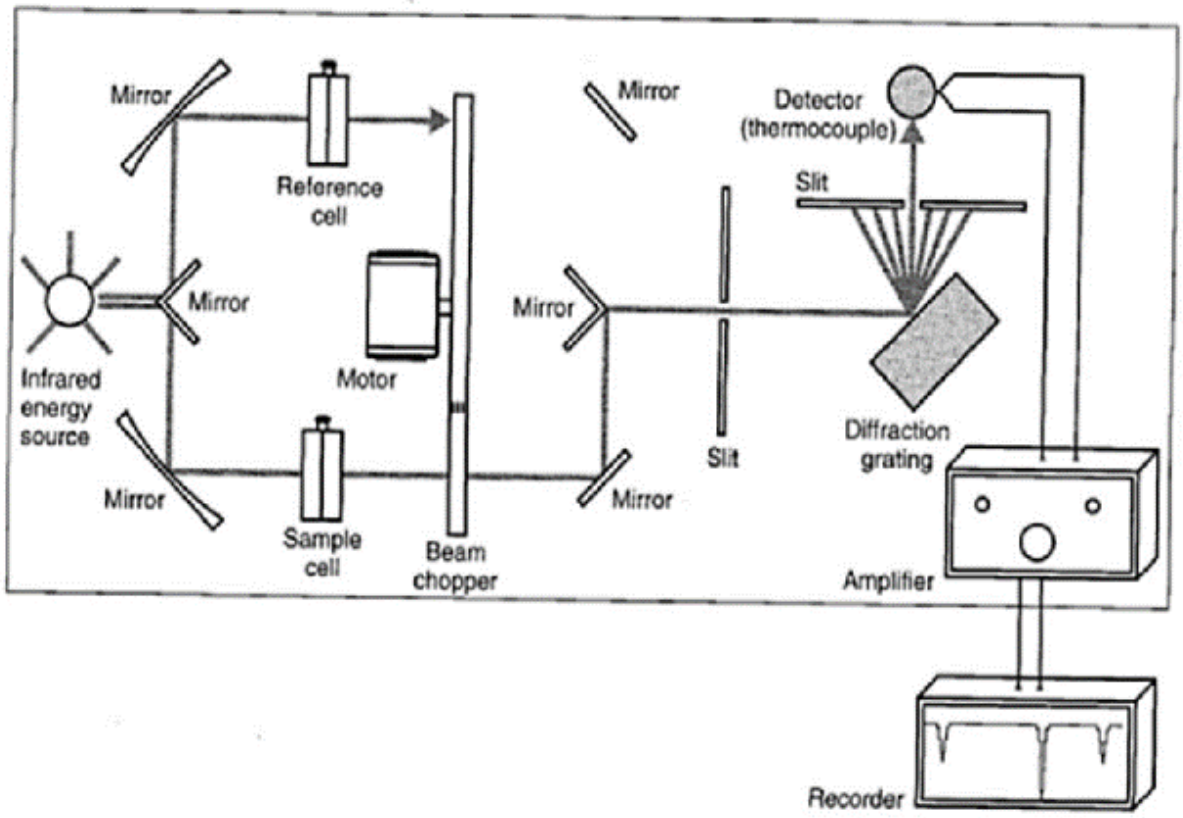

Figure 5(b). Schematic diagram of an infrared spectrophotometer [69]

3.2. Thermal Characterization: Thermo-analytical techniques offer a well-established methodology for researching the thermodynamics of numerous processes involved in a wide range of sectors encompassing both industry and research, as well as for thermal characterisation of materials. With these methods, the sample being studied is put through a predetermined cycle of heat, cool, and isothermal phases in a furnace's-controlled environment. Accurate measurements are taken of the changes that take place in various parameters of interest in a relation to temperature and pressure. The physico-chemical processes that occur with temperature are characterised by the profiles of these parameters. Many thermal analysis tools are used in various fields of materials science, chemistry, and metallurgical and chemical engineering [70-71]. Some of the widely used thermal techniques are listed below. DTA –Measures temperature excursion of sample [variable – dT/dt], DSC – Measures heal flow into or out of sample [variable – dH/dt], TGA –Measures sample weight change with temperature [variable – m; dm/dt], TMA – Measures change in physical dimensions of sample as a function of temperature [Variable – L; dL/dt], The measurement of the parameters of a material in this manner give valuable information regarding-Purity determination, Oxidative stability, Melting/crystallization behavior, Glass transitions, Solid-solid and liquid transitions, Phase transition and Morphology, Polymorphism, Crystalline Amorphous, Degree of Crystallinity, Cross-linking reactions, Specific heat, Thermo kinetics, Decomposition in Liquid Crystal Glass-ceramics polymers, Among different thermal techniques DSC would be described as it has been used practically in the present work.

3.2.1. Differential Scanning Calorimetry (DSC):

It is challenging to get quantitative information about the sample or heat of transition with conventional DTA, but it can provide strong qualitative information about temperature and a transition sign. The significance of usually

unidentified variables, such as the sample's specific heat and thermal conductivities before and after the transition, contributes to this challenge. The region beneath the endotherm or exotherm is further influenced by the rate of heating, thermocouple location, and other instrumental characteristics. By transforming the DTA apparatus's sample container into a differential scanning calorimeter, quantitative data can be achieved. An experimental method for determining the energy required creating an almost zero temperature difference between a test substance S (and its reaction products) and an inert reference material R is called differential scanning calorimetry, or DSC.

This is done by exposing the two samples to the same (heating, cooling, or constant) temperature programme. The term DSC originated from this technology, which detects energy directly and allows precise measurements of heat capacity [72–73] (figure 6).

The temperatures of the specimen (TS) and reference (TR) in power-compensation DSC are controlled independently using distinct yet identical ovens. The sample and reference temperatures are kept at zero by varying the power delivered to the two furnaces. This approach determines the changes in enthalpy or heat capacity between the test sample S and the standard R. Conversely, in Heat-flux DSC, a high thermal conductivity metallic block ensures efficient heat transfer between S and R within the same furnace as the test sample S and standard material R, typically an empty sample pan and lid. Variations in temperature compared to R are induced by alterations in the enthalpy or heat capacity of the specimen S. Because of the excellent thermal contact between S and R, this leads to a certain heat-flow between S and R, albeit one that is smaller than those in DTA.

Calibration experiments are used to record the temperature differential (DT) between S and R and then connect it to the enthalpy change in the specimen. The only significant distinction between the heat-flux DSC system and the DTA system is the improved heat-flow channel connecting the reference and specimen

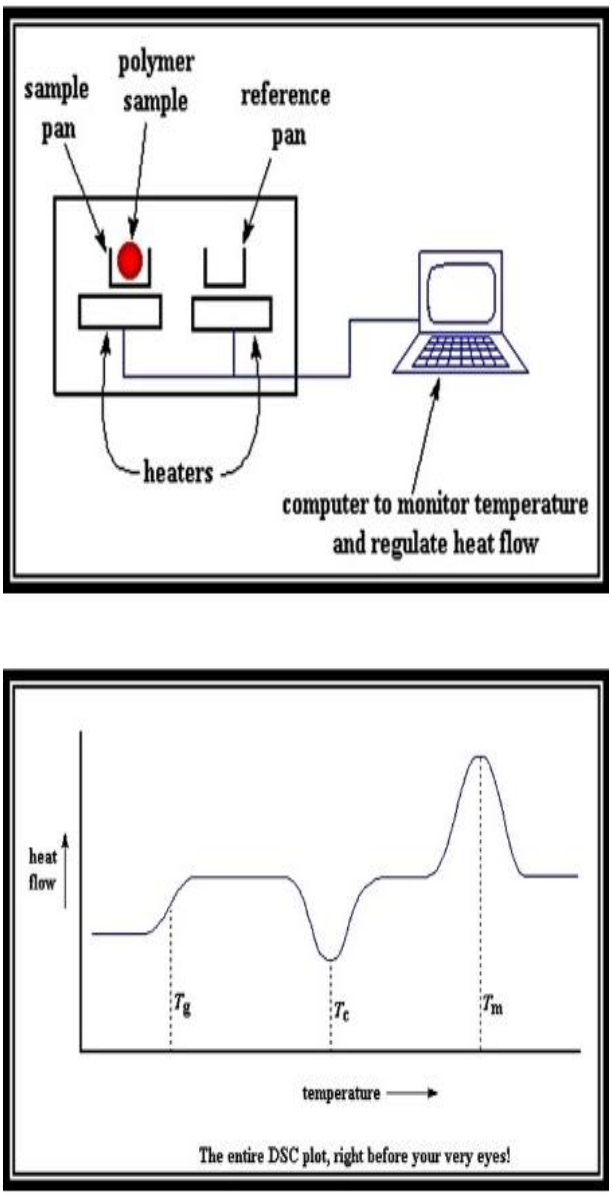

Figure 6. Block diagram Heat Flow DSC [74]

crucibles. DSC is primarily used to examine phase transitions, including exothermic decompositions, melting, and glass transitions. These transitions entail changes in energy or heat capacity, which are highly sensitively detectable by DSC. The fundamental idea behind this technique is that, to keep the reference and sample at the same temperature during a physical change like a phase transition, heat will need to enter the sample. Whether the process is exothermic or endothermic determines how much heat must flow to the sample. For instance, when a solid sample melts into a liquid, more heat must enter the sample for its temperature to rise at

the same rate as the reference. When the sample absorbs heat during an endothermic phase change from a solid to a liquid, this event takes place. Similarly, during exothermic reactions like crystallisation, less heat is needed to raise the sample's temperature. Differential scanning calorimeters can quantify the heat received or emitted during these transitions by measuring the difference in heat flow between the sample and a reference. Glass transitions and other nuances in phase changes can be observed with DSC. Because of its usefulness in assessing sample purity and researching polymer curing, it is frequently utilised in industry as a quality control device. Glass transitions may occur when the temperature of an amorphous solid is elevated. These shifts manifest as a step in the DSC signal's recorded baseline. There isn't a formal phase transition; instead, the sample's heat capacity changes as a result. An amorphous solid will become less viscous as the temperature rises. The molecules might eventually become mobile enough to spontaneously organise into a crystalline structure. We call this crystallisation (Tc). The DSC curve signal peaks because of this exothermic process, which turns the amorphous solid into a crystalline solid. The sample finally achieves its melting temperature (Tm) as the temperature rises. An endothermic peak can be seen on the DSC because of melting. To create phase diagrams for a variety of chemical systems, DSC is a crucial technique due to its capacity to assure transition temperatures and enthalpies.DSC is more limited in its upper operating temperature range (~ 800°C) than DTA, due to increasing thermal emissivity as temperature rises. This effect reduces calorimetric sensitivity and makes high temperature calibration difficult. Sample can be cooled to near liquid nitrogen temperature, which makes this an ideal technique for detecting this low temperature glass and sub-glass transitions in polymers. In DSC, sample encapsulation is extremely important. Sample can be hermetically sealed in pairs with 2-3 atmosphere bursting pressure either with maximum value or with minimum volume. When a volatile sample is used, these pans may burst at different times and bursting time may be dependent on sample size. Volatile sample in crimped (c and d) or open (e) pan will also show variable effects. In addition, parameters that can be studied in DTA, DSC can also be used to study many more parameters related to enthalpy changes and kinetics of phenomenon of material under study. Furthermore, physical phenomenon like determination of phase diagram of polymer substance, monomer purity, glass transition, fractional crystallinity, identification of crystalline phase present, liquid crystalline transition in both main or side chain of polymer, metal-stable equilibrium, free versus bound water in polymer, ferroelectric transition, effect of orientation salting out or salting in and many more parameters can be studied through DSC measurements.

3.3. Electrochemical Studies:

3.3.1. Cyclic Voltammetry Studies:

Verifying the material's electrochemical and window stability is crucial for the electrochemical device applications of nanocomposite polymer electrolytes. offers a wide range of potent voltametric and coulometric techniques for basic research on electrochemical reactions. These techniques are based on sensitive computer-controlled potentiostates and a variety of innovative stationary electrodes and microelectrodes. One of these new techniques that is most useful is cyclic voltammetry (CV), which is widely used in organic, inorganic, and materials research. It is frequently the first experiment conducted in an electrochemical study [75]. Electrochemical measurements of a general purpose are the objective of the Model 600D series CV instrument. The schematic displayed in Figure 7 below illustrates the structure of the device. Components of the system include rapid data acquisition circuitry, a high-speed digital function generator, Potentio stat, and Galvano stat (available in specific models). The device provides a current range of ±250 mA and a potential control range of ±10 V. Currents as low as tens of pico-amperes can be detected by it. It is possible to measure a 10 μm disc

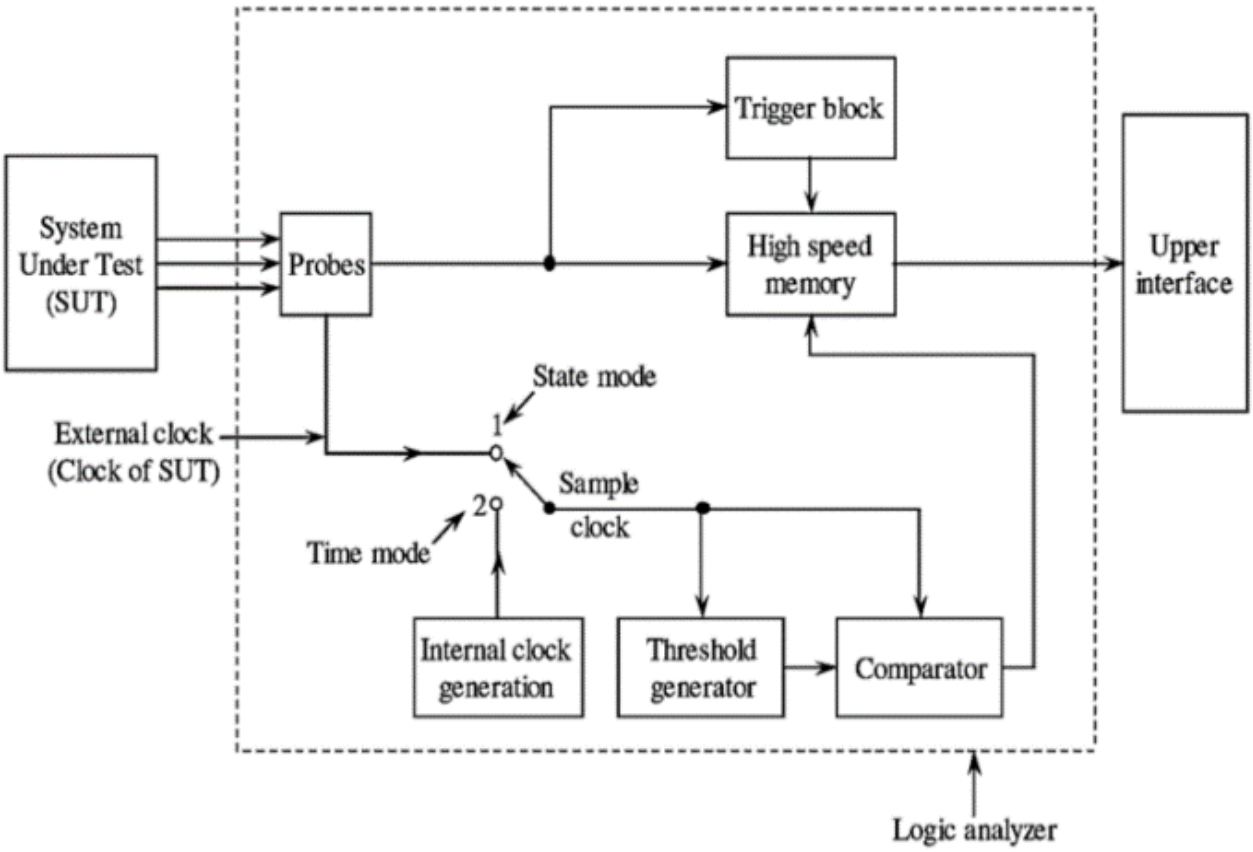

Figure 7(a). Block diagram of CH analyzer Instrument [76]

electrode's steady-state current precisely without the use of external adapters. Currents as low as 1 pA can be measured with the fully automated CHI200B Pico-amp Booster and Faraday Cage, which are compatible with the CHI600D series. The instruments demonstrate high speed capabilities with a function generator that may update at a rate of 10 MHz and a maximum sampling rate of 1 MHz at a resolution of 16 bits. This apparatus offers a wide dynamic range over multiple experimental time frames. In cyclic voltammetry, for illustration, the scan rate can be as high as 1000 V/s with a 0.1 mV potential increment or as high as 5000 V/s with a 1 mV potential increment. With its 4-electrode configuration, the Potentiostat/Galvanostat can be used for liquid-liquid interface measurements and reduces the influence of contact resistance in connections and relays when doing high current tests. The data acquisition systems provide the simultaneous recording of electrochemical data and external input signals, such as spectroscopic signals. The gadget will instantly reset the voltage and current to zero, removing the requirement for routine recalibration. Additionally, it has an authentic integrator chronocoulometric to analyse samples of polymer electrolyte under polarisation. When operating as a bipotentiostat, the second channel can be configured to maintain a constant independent voltage, replicate the voltage of the first channel, or sustain a consistent voltage differential. This additional channel accommodates various voltametric and amperometry techniques, as well as advanced electrochemical workstations and comprehensive electrochemical analyzers. This apparatus offers a range of electrochemical methods, a built-in digital CV simulator, and a program for simulating and fitting impedance. These capabilities offer robust resources for conducting both in-depth studies on electrochemical mechanisms and meticulous analysis of trace elements. The objective of utilizing this method is to thoroughly evaluate the effectiveness and

limitations of this waveform in elucidating electrode reaction mechanisms. The schematic diagram and computer-managed CH workstation are depicted in figure-7a.

Information about the stability and reaction kinetics of these electro-generated species can be obtained from the oxidation and reduction of chemical species at the electrode surface. One method of measuring is the cyclic voltammogram. Three peak currents are measured: the anodic peak current (ipa), the cathodic peak potential (E_{pc}), and the cathodic peak current (i_{pc}). These peak potentials provide information on the analyte's identity as well as the oxidation/reduction process's kinetics in electrolyte systems. Peak current providing data on the stability and analysis concentration of the electro-generated species. A pair of stable chemical compounds that interchange quickly and kinetically when the applied voltage changes at the electrode electrolyte surface is known as an electrochemical reversible redox couple [77]. The formal reduction potential (E°) for a reversible couple is determined by averaging the anodic and cathodic peak potentials, expressed by the following relation:

$$E^o = \frac{E_{pa} + E_{pc}}{2} \quad \ldots\ldots\ldots\ldots (7)$$

The degree of separation between the anodic and cathodic peak potentials can be expressed as the number of ions, n, transported during the kinetics of an electrochemically reversible reaction. This relation can be found here.

$$\Delta E_p = E_{pa} - E_{pc} = \frac{0.0592V}{n} \quad \ldots\ldots\ldots\ldots (8)$$

A cyclic voltagram with a peak separation of 0.0592 V is ideal for this reaction. By using the Randles-Sevcik equation, the cyclic voltagram's peak current magnitude can reveal information about the analyte's concentration.

$$i_p = (2.69 \times 10^5) n^{3/2} A D^{1/2} C V^{1/2} \quad \ldots\ldots\ldots (9)$$

where,

i_p = peak current, n=electron stoichiometry, eq/mol A =electrode area (cm^2), D=diffusion coefficient, cm^2/s, C = concentration, mol/cm^3, v = scan rate, V/s, in above equation, a peak current increase with square root of the scan rate and is directly proportional to concentration. The values of i_{pa} and i_{pc} should be close for a simple reversible couple. *i.e.*

$$\frac{i_{pa}}{i_{pc}} = 1 \quad \ldots\ldots\ldots\ldots (10)$$

If species are generated electrochemically and further chemical reactions take place, the peak current ratio can differ considerably from the predicted value. When waves are semi-reversible in CV the peak current ratio is less than or greater than 1, Figure 7b.

One can estimate ion insertion and extraction can be from the peak area. The area (\(A_i \)) enclosed by each cycle shows the quantity of ion inclusion in the polymeric chain.With the help of observation of the area under the CV peak, the cycle efficiency (Q_i) of electrolytic materials can be evaluated from below equation [78].

$$Q_i = \frac{A_i}{A_1} \quad \ldots\ldots\ldots\ldots (11)$$

Where Q_i *is* the cycle efficiency, A_1 is the area of the first cycle curve A_i the area of i^{th} cycle curve.

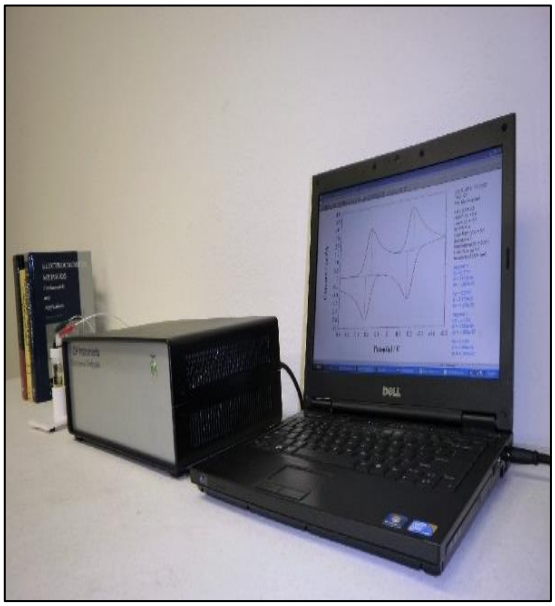

Figure 7(b). Computer controlled CH Workstation

3.4. Electrical Characterization:

3.4.1. Ion Transport Studies:

Ion dynamics of any electrolyte should be well understood before inducting them to any electro-chemical device application. Electrolytes of any form (solid/liquid/semisolid-gel) possess overall electro-neutrality but the ions are free to perform, Brownian motion resulting in net zero current. When electrolyte is subjected to electric field, these random mobile ions start drifting in certain direction viz. direction of electric field leading to conduction of ion. Ion transport dynamics can be understood macroscopically or microscopically. Microscopic ion dynamics corresponds to understanding the mechanism of ion transport at molecular/atomic level in the impact of applied electric field. Macroscopic behavior on the other hand concerns all change in concentration(s) of ion species (s) (or all type of ions) within a specific volume or ion transport through a particular cross-sectional area and it provides property of bulk. Commonly used macroscopic ion transport properties are conductivity, mobility of ionic species, ionic transference number and activation energy. To assess these properties the techniques used in present studies are discussed below.

3.4.2. Transference Number:

The ratio of current produced by ionic species migration, Ii, to the total current resulting from all conducting species, or t_i, is known.

$$t_i = \frac{I_i}{I_t} \dots\dots\dots\dots (12)$$

If we assume σ_i to be the conductivity due to all type of ions and σ_t the total conductivity encompassing ionic as well as electronic parts ($\sigma_t = \sigma_i + \sigma_e$) then ionic transference number can also be expressed as

$$t_i = \frac{\sigma_{ions}}{\sigma_{total}} = \frac{i_{ions}}{i_{total}} \dots\dots\dots\dots\dots (13)$$

In case of superionic solids, it is essential to know separately the cationic contribution (t_{cation}) and anionic contribution (t_{anion}) to total transference number t_{ion} as well.Amongst the different techniques of ionic transference number (t_{ion}) measurement applicable to polymer nanocomposite electrolyte, *dc* polarization technique has been employed in present investigation. The dc polarization technique is also known as Wagner polarisation after the name of J.B. Wagner and C. Wagner [79]. This approach, as shown in figure-8(a), applies a dc voltage below the material's breakdown potential across the sample, which is sandwiched between two blocking electrodes. The time variation of the current through the sample is subsequently recorded. Upon activating the power supply, the total current flowing through the sample experiences a rapid initial reduction due to polarisation at the electrode electrolyte interface. Eventually, the current achieves a residual constant value, as shown in Figure 8(b). Both the ionic and electronic contributions to conductivity are responsible for the initial current.

($\sigma_t = \sigma_i + \sigma_e$) whereas constant current is only due to electronic contribution (σ_e). The t_{ion}can obviously be determined by equation (2.11).

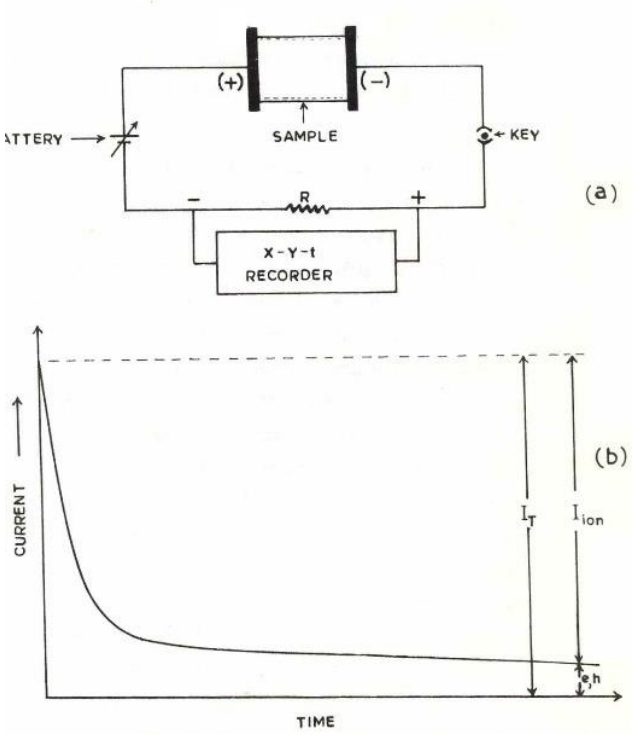

Figure -8 Schematic experimental arrangement for ionic transference number measurement using wager's DC Polarization Method (a)Blocking Electrodes (b)Typical Current vs Time Plot [80]

Though Wagner polarization method is simple to assess t_{ion} it is difficult to assess the type of charge carrier responsible for conduction i.e. anion or cation or both. Further, when electrode electrolyte interface resistance becomes comparable or more than bulk electrolyte, the residual electronic current may lead to incorrect determination of t_{ion}. Non-availability of perfect/non-blocking electrodes for proton conducting materials and inability to determine transference number of gaseous species further reduces the potential of this method. Nevertheless, a rough estimate of ionic nature of material can be made through this technique. The relationship between the initial current ($i_{initial}$) and final current (i_{final}) obtained from the I-t plots is used to compute the total ionic transference number (t_{ion}).

$$t_{ion} = \frac{i_{initial} - i_{final}}{i_{initial}} \quad \ldots\ldots\ldots\ldots\ldots (14)$$

3.5. Bulk Ionic Conductivity:

The most useful parameter associated with composite polymer gel electrolytes is its DC ionic conductivity and its variation as function of temperature and composition. This electrical parameter influences the power density of electrochemical devices and establishes the mass transport rate across the electrolyte. Therefore, conductivity of electrolyte is of prime concern itself and equal to inverse of resistivity. Section 2.3 lists some techniques of conductivity measurement of ionic conductors. Two terminal *dc* techniques are most simple but at the interface, partial blocking of ionic current leads to build up of space charge which poses problem in estimation of bulk conductivity [81,82]. Hence this charge builds up makes conductivity time dependent quantity which means σ corresponds to the value at which interval it is measured. Use of reversible electrode technique resolves the problem up to some extent by yielding consistent results but it creates error in assessing conductivity value of electrolyte precisely due to slow oxidation reduction process at the interfaces. In addition, it is often difficult to obtain good reversible electrodes possessing wide temperature window. Further, four probe cell is difficult to construct. Two terminal ac signal method with only one stimulus signal frequency is yet another easy way of determining conductivities of samples and generally it provides sufficiently accurate conductivity values. A four-probe ac configuration with independent current and voltage leads can be utilised when there is a significant charge transfer impedance. However, this approach is insufficient to accurately and completely characterise nanocomposite polymer electrolytes. The ultimate impedance of a cell is influenced by multiple factors. Because of their widely differing relaxation times, the contributions from the Charge transfer across the interface, the resulting double layer capacitance, the electrode-electrolyte interface impedance, and the movement of ions through the bulk of the electrolyte are all summed in a single frequency and respond quite differently in different frequency ranges. Heterogeneous distribution of phases in polymer electrolyte result in varying concentration gradient and grain boundaries which further complicates the situation. A common behavior of solid electrolyte conductivity (in logσ) with frequency (log f) is shown in figure-9.

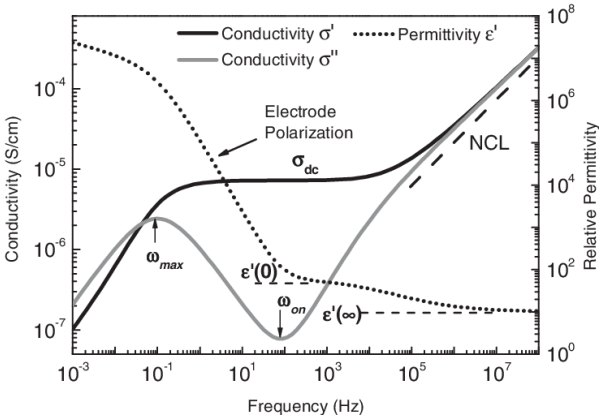

Figure -9 Variation in Conductivity with Frequency of Applied Field [83]

At very low frequencies, the electrode effects are pre-dominant. At intermediate frequency, the value corresponding to the plateau is usually taken as true *dc* conductivity. Therefore, measurement of frequency dependent conductivity or impedance is necessary to realize individual contribution.

Impedance spectroscopic technique—an ac technique with a wide range of frequency of measurement—was developed because of the systematic study of the ac response of an electrolyte or an electrochemical cell made feasible by technological and electrochemical advancements throughout time [84–85].

3.6. Impedance Spectroscopy:

Impedance spectroscopy gives range of information on electrical and other physio-chemical properties of the material and interface with their inter-relationship. Baureale [86] was the first to apply this technique for study of zirconia based solid electrolytes. In this technique, impedance is measured over a suitable frequency range. The collected data can be utilised to study the dynamics of bound and mobile charges in the bulk and interfacial area. Measurements of complex entities such as Complex impedance (Z*), complex permittivity (ε*), complex modulus (M*), and complex admittance (Y*) are all included in the scope of impedance spectroscopy. A basic formalisation of these factors and their relationships is provided in Table 2.2. Amongst these, the most common complex quantity- impedance Z* can be written as

$$Z^*(\omega) = Z'(\omega) - jZ''(\omega) \ldots\ldots\ldots (15)$$

where Z' and Z" are the real and imaginary part of impedance for simple equivalent parallel RC combination

$$Z^* = R(s) - j\omega CS \ldots\ldots\ldots (16)$$

Instead of plotting impedance Z* versus frequency, real and imaginary parts of impedance are commonly plotted as parametric function of frequency. This plot describes circular areas, which are characteristic of cell under investigation. Each of the physical process taking places in an electrochemical cell would give separate semi-circle provided their relaxation times are widely different. Theoretically, five semicircular arcs have been proposed but experimentally only three semi-circles are commonly observed [87] (figure-10).

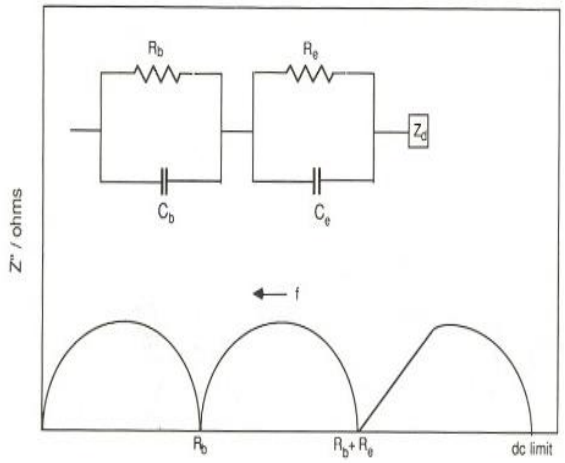

Figure -10 A typical complex plane lot and idealized circuit for a polymer electrolyte cell (non-blocking electrode for cations). R_e electrode resistance; C_e electrode capacitance R_b electrolyte resistance; C_b bulk geometric capacitance; $Z_d$diffusion-controlled impedance

The complex impedance plots of few basic circuit elements and their elementary combinations are represented in figure-11 (a) and (b).

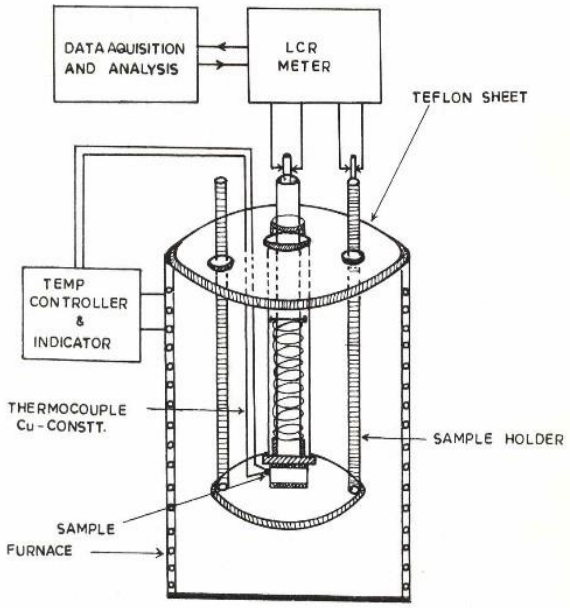

Figure -11(a) Experimental assembly used in impedance measurement for assessment of bulk ionic conductivity and dielectric parameters [88]

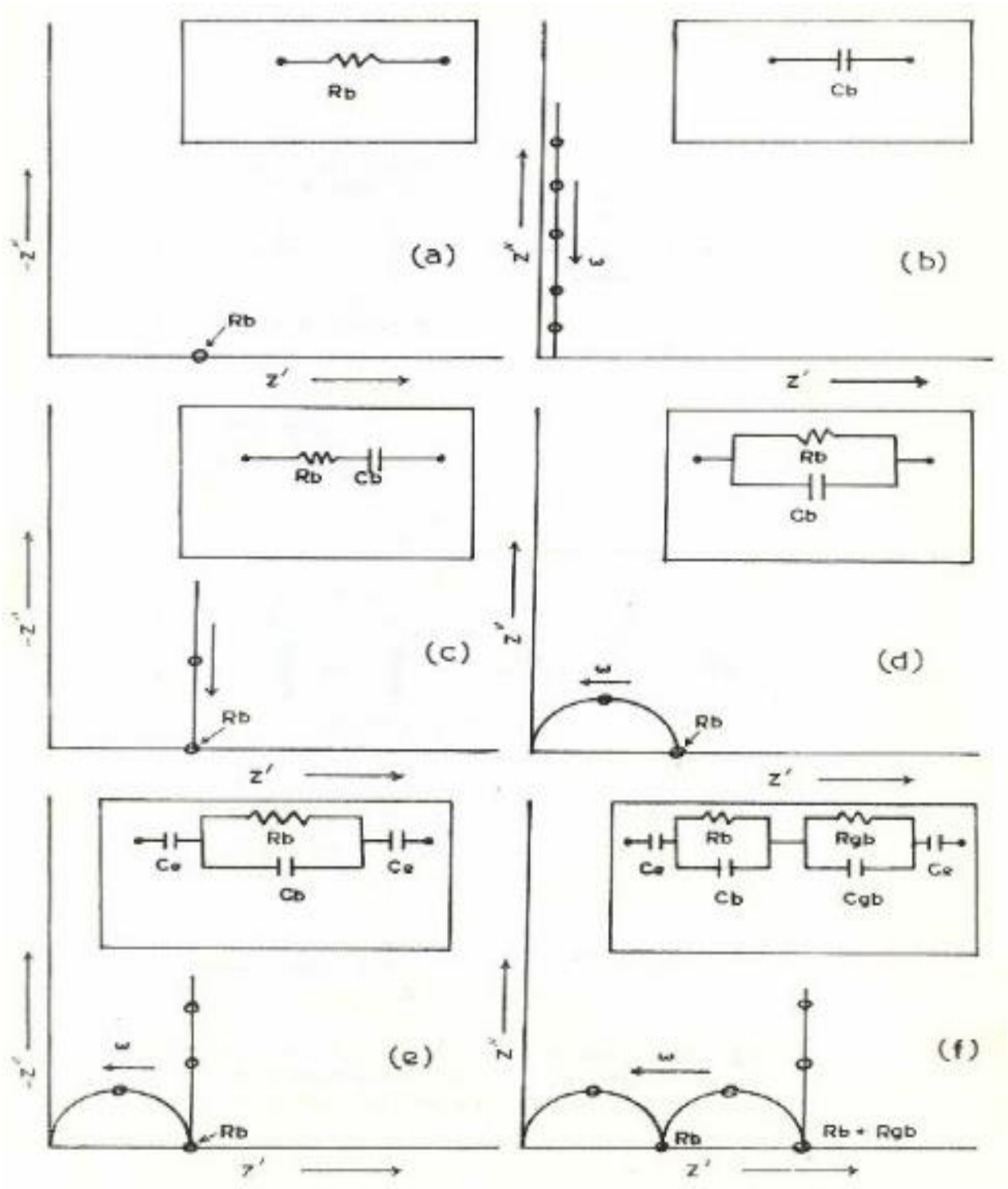

Figure 11(b). Complex impedance plots for some elementary circuit elements (a) R (b) C and (c-f) their combinations (circuits are shown in inset)

To the first approximation, each of the semicircles in the impedance diagram may be considered as the response of a lumped RC combination. From the correlation between the semicircle parameter and R and C components, the plotting of such diagrams provides straightforward determination of electrolyte resistance whatever may be the degree of electrolyte polarization. One of the biggest advantages of this method is that it does not require the use of reversible electrodes or complicated cell geometry. The equivalent circuit and impedance plot of an elementary cell with blocking as well as non-

blocking electrode is shown in figure-12. The intercept of first semicircle (high frequency) to real axis represents bulk resistance, R_b (figure-12 (a) and thus conductivity can be obviously evaluated by the relation

$$\sigma = \frac{l}{R_a A} \ldots\ldots\ldots (17)$$

where, R_a is the bulk resistance of sample, *l*= thickness of the sample under study and A =the cross-section area of sample under study.

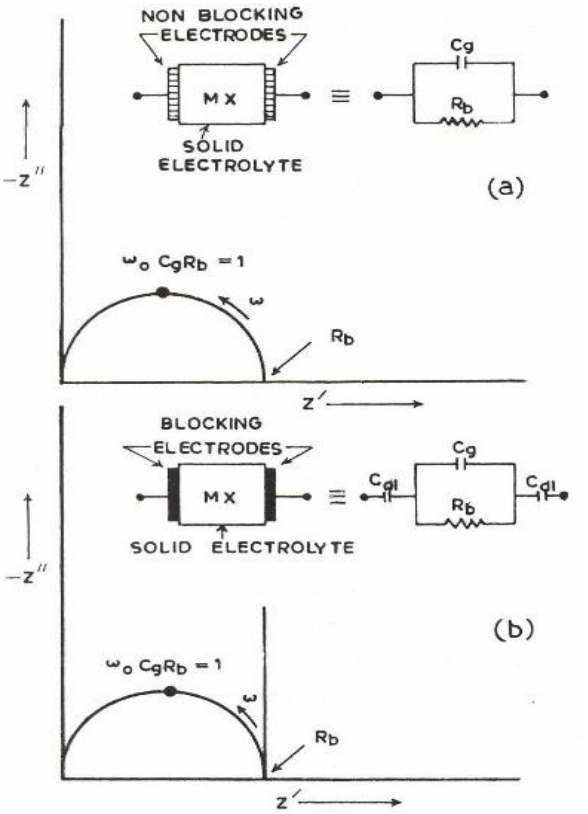

Figure 12. Complex impedance plots for typical electrochemical cells along with their equivalent circuits (a) with non-blocking electrodes and (b) with blocking electrodes

Sometimes it is challenging to resolve highly complex contributions of lines and semicircles in an impedance graphic. In such condition the admittance diagram is preferred because identification of deviation from straight line is easier than that from circular arc. In the present work, polymer composite polymer electrolytes have been sandwiched between two blocking platinum electrodes and kept in spring loaded holder as shown in figure-12 (b). The impedance measurements (Z,θ) have been performed on a Hioki make LCR meter (coupled to a computer) between a frequency range 40 Hz – 100 KHz.

Some Additional Features

Second Semicircle – Polymer electrolytes contain crystalline as well as amorphous regions along with uneven salt distribution throughout the matrix. Conductivity in such a system is a combination of inter grain and intra grain conduction. Because of the high defect density in the interface region, the grain boundaries may both provide high conductivity and impede ion movement. In such a case, a second semicircle is observed after the semicircle of ion conduction and polarization [89, 90]. The grain boundaries may be expressed as combinations of two parallel RC elements representing inter and intra granular regions (figure-13(b)).

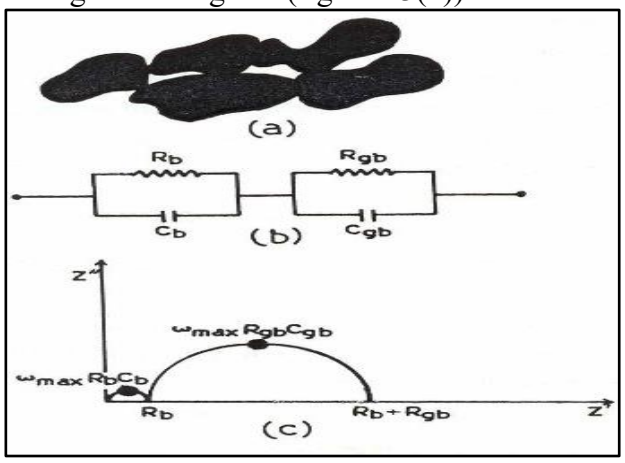

Figure – 13 (a) Approximate representation of in homogenous polymer electrolyte with individual grains in contact at grain boundary (b) equivalent circuit for (c) complex impedance plot for circuit

If conductivity increases at the grain boundary, it will give an apparent bulk resistance that is lower than real bulk effect.

Identification of Semicircle - The entire semicircles are rarely obtained within observation range. It may be then difficult to identify the semicircle arising from phenomenon. However, some tricks outlined below are used in proper identification

i. As a rule, the observation range shift from left to right of impedance diagram as the temperature increases. Bulk properties are

usually observed at low temperature and electrode characteristics appear at high temperatures.

ii. Since bulk resistance depends upon the length of sample and hence real intercept corresponds to bulk resistance in the impedance plot. Therefore, to separate bulk property, semicircle from electrode semicircle, measurements should be repeated for different length of sample.

iii. Replacement of electrode material can also be used to obtain electrode semicircle changes. Similarly, relaxation frequencies are dimension independent and thus measurement of relaxation frequency of concerned semicircle (i.e. top of semicircle) may also provide differentiation.

iv. Since bulk properties are found to be perfectly linear and relevant part of $Z^{'}$ $Z^{''}$ plot are independent of amplitude of applied signal whereas electrode response with amplitude variation is not linear especially for voltages greater than 100 mV. Therefore, variation in amplitude of applied signal may also be helpful in justification of processes.

v. Determination of capacitance and related dielectric constant may also provide identification criterion.

Overlapping of Semicircles – As discussed earlier, the plots of real and imaginary component will show one semicircle for each process taking place in the cell under study. If the relaxation time for each process differs by 100 times, separate semicircle would be observed. But in most cases considerable overlapping of semicircle may occur. To resolve this problem frequency distribution can be checked by Cole-Cole approach [91]. In this technique distances (u and v) are measured from origin and real axis intercept as shown in figure-14.

Logarithm of u/v is graphed as a function of frequency to decide the number of processes. Over the years, computers have been employed for analysis of overlapping semicircles.

Warburg Resistance – Nevertheless, difficulties occur when attempting to obtain the analogous circuit for the purpose of simulating the electrode phenomena in the cell.

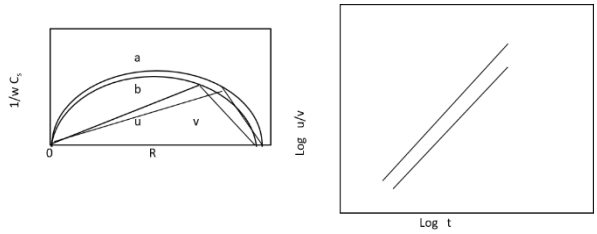

Figure-14 Cole- Cole method analyzing the overlapping semicircle [92]

The component that explains the impedance resulting from several electrode processes—namely, charge transfer, diffusion steps, and double layer capacitance (Cdl)—must be included. A transfer resistance Rt can be used to characterise the charge transfer resistance since the current is in phase with the applied voltage. It often corresponds with the electrode reaction rate. The concentration independent diffusion term is a function of frequency because at high frequencies the bulky ions move too slowly to react in phase with applied potential [93–94]. A straightforward formula for the interfacial impedance of the working electrode:

$$Z = \left[i\omega C_{dl} + \frac{1}{(Rt + W)} \right]^{-1} \dots\dots\dots\dots (18)$$

Where W, the Warburg impedance is given by

$$W = S\omega^{1/2} - js\omega^{1/2} \dots\dots\dots (19)$$

The Warburg coefficient S is a function of concentration and diffusion of oxidized and reduced species.

Constant Phase (angle) Element (CPE)-In many cases, especially in polymer composite gel electrolytes, depression of high frequency semicircle and bending of low frequency spike towards real axis are observed. The depression angle is usually small for bulk semicircle but can be very large for electrode semicircle. This feature cannot be manipulated with series and parallel combination of R & C component. A new type of circuit element is proposed and termed as constant phase angle element (CPE)

to account for displacement of centre of semicircle below real axis and spike tilting. The value of this impedance Z_{CPE} is given by

$$Z_{CPE} = k(j\omega)^{-p} \quad \text{where } 0 \leq p \leq 1 \quad \ldots\ldots\ldots(20)$$

When p = 0, Z = independent of frequency K = just a resistance R and p = 1, $Z = \frac{k}{j\omega} = \frac{-j}{\omega k^{-1}}$; the constant k^{-1} now corresponding to the capacitance C. The CPE functions as an intermediary between a resistor and a capacitor when p is between 0 and 1 (as is typically encountered). Thus, CPE connected in parallel with bulk resistance will result in depressed semicircle (figure-15).

Several interpretations have been proposed to explain this phenomenon. A general explanation can be offered in terms of inter and intra grain heterogeneity [88]. In case of polymer electrolytes, this may be due to distribution of crystalline non-conducting phase within conducting amorphous phase. Thus, heterogeneity in properties and their statistical distribution of corresponding relaxation may be the reason. Johnscher [96] have considered this semicircle depression as a specific property of ionic conductor and dielectric material. According to him, it is an essential attribute of the elementary jump of ion and due to local energy storage effect associated with slow relaxation of polarization, which is induced by mobile ions within its surroundings. Further, tilting of low frequency spike is related to the roughness of electrode-electrolyte interfaces. Series combination of CPE and bulk resistance represents this tilted low frequency spike. The bulk resistance is obtained from the intersection of flattened semicircle and tilted spike.

3.7. Dielectric Spectroscopy:

Dielectric spectroscopy establishes a connection between the features of the bulk properties of the material under study and the attributes of each individual constituent. The trend of frequency dependent dielectric studies, started during the days of Cole and Cole [97], have been spread over a wide variety of solid-state material characterization,

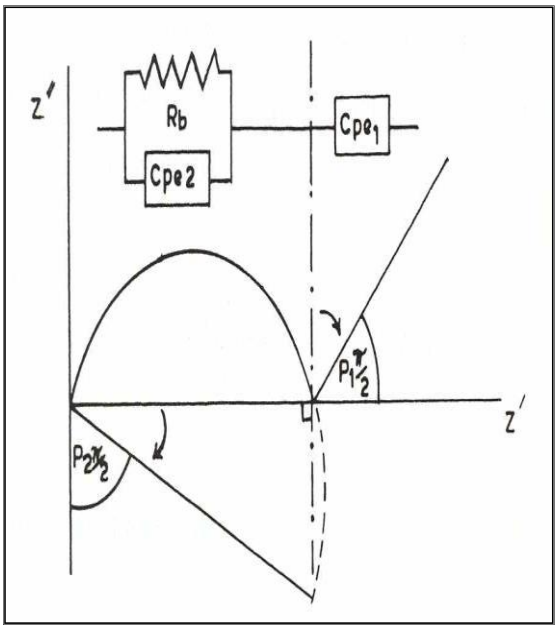

Figure-15 Constant phase element response of a typical polymer electrolyte cell illustrating depression of semicircle and tilting of spike. [95]

including, ion conducting materials. Several dipolar relaxations may be of interest in polymer-based electrolytes such as dipolar, segmental, and larger unit relaxation in the polymer itself and relaxation due to complexation with salt/acid (i.e. dipoles formed on complexation cation-anion pairs), relaxation due to clusters etc. The kind and type of ionic and molecular motions and their interactions, which are influenced by the chemical composition, molecular structure, and morphology of the sample under examination, are abundantly revealed by studying relaxation processes in such materials [98–99]. The relaxation frequency and the strength of relaxation are characteristic of the relaxing dipole. Therefore, the measurement of relaxation time can be used to differentiate conductivity relaxation processes from dipolar relaxation within the bulk materials. Despite being significant and helpful from a scientific perspective, dielectric investigations on ionically conducting solid nanocomposite polymer electrolyte have not been thoroughly investigated because of data analysis limitations and complexity. Fontenella et al. [100–101] have described the low frequency dielectric properties of a pure

polymer (PEO, PPO) and their complexes with different salts. The dielectric characteristics of ionically conducting solid polymeric films have also been reported recently [102-103] by Elisasson et al. [104]. While many research groups have done a good deal of work on the synthesis and characterisation of NCPEs [105, 106], relatively few studies have been published on the dielectric attributes of NCPEs to far. Impedance spectroscopy was used to analyse the electrical properties of NCPE films when a 200 mV small alternating current was applied across a symmetrical cell of the type Pt // NCPE // Pt (where Pt is for platinum blocking electrodes). A computer-controlled impedance analyzer (HIOKI LCR Hi-Tester, model: 3520, Japan) was used to get complex impedance parameters, or impedance, permittivity, and tangent loss parameters, as a function of frequency (40Hz to 100 KHz) at different temperatures (RT to 100°C). Relation 15 was utilised to compute the real and imaginary parts of impedance and permittivity.

$$\varepsilon * = \varepsilon' - j\varepsilon'' \ldots\ldots\ldots\ldots\ldots\ldots (21)$$

$$\varepsilon' = \frac{-Z''}{\omega C_o\left(Z'^2 + Z''^2\right)} \ldots\ldots\ldots\ldots\ldots (22)$$

$$\varepsilon'' = \frac{Z'}{\omega C_o\left(Z'^2 + Z''^2\right)} \ldots\ldots\ldots\ldots\ldots (23)$$

Where

ω= the angular frequency, C_o= the geometrical capacitance in vacuum of the same dimension as the

Sample [Co $= \frac{0.0885A}{d} PF$], A= the area of electrode and d = the thickness of the sample. The a. c. conductivity was evaluated from dielectric data in accordance with the relation

$$\sigma_{ac} = \omega \varepsilon_o \varepsilon_r \tan\delta \ldots\ldots\ldots\ldots\ldots\ldots (24)$$

Where $\varepsilon_r = \frac{C}{C_o}$ is the relative permittivity ω= 2πf, f= the frequency of the applied field, Following relation can be used to evaluate the tangent loss:

$$\tau \alpha \vartheta \delta \frac{\varepsilon''}{\varepsilon'} = \frac{Z''}{Z'} \ldots\ldots\ldots\ldots\ldots (25)$$

For different nanocomposite polymer electrolytes, the change of σ_{ac} with frequency displays dispersion at higher frequencies and a frequency independent tiny plateau in the low frequency zone. The universal power law governs this behaviour .

$$\sigma_{\alpha\gamma}(\omega) = \sigma_o + A\omega^{\vartheta} \ldots\ldots\ldots\ldots\ldots (26)$$

Where,

σ_o = d.c. conductivity (frequency independent plateau in the low frequency region)

A= the pre-exponential factor and,

n = the fractional exponent between 0 and 1.

The electrode polarisation effect is the cause of the conductivity spectrum's divergence from the plateau region (σ_{dc}) value in the low frequency zone. Through fitting of the observed to relation 26, the values of σ_o, A, and n were determined. Power law exponents (n) for ionic conductors typically vary from 1 to 0.5, denoting diffusion-limited hopping (tortuous paths) and optimal long-range pathways, respectively [107]. The universal dynamic response [108], which has been extensively noted in disorganised materials including Doped crystalline solids, ionically conducting glasses [109], and conducting polymers [110], as well as in general, follows the general behaviour of AC. It is generally accepted that this behaviour is demonstrated in the mechanism of charge transport nature of charge carriers.

In ac conductivity, it is observed that the frequency dependence of conductivity can be split into three zones:

(i) a plateau area of low frequency; (ii) an area of intermediate frequency dispersion. (iii) high frequency area that is not reliant on frequency Because of electrode polarisation effects at the interfaces between the electrode and the electrolyte, conductivity is nearly frequency independent in the low frequency range [111]. High frequency dispersion is indicated by the conductivity in the intermediate frequency band, which varies greatly with frequency. The conductivity increases with frequency in this zone, which is closer to relaxation times, due to the high mobility of charge carriers; in contrast, the

conductivity once more becomes frequency independent in the third high frequency region. The fact that the charge carriers are not sufficiently free to follow the fluctuating electric field in this location demonstrates that conductivity is practically frequency independent despite the high frequency.The Cole–Cole expression, or real part (ε') against imaginary part (ε") of complex permittivity, can be used to characterise the dielectric behaviour of polymeric materials [112]. The centre of the semicircular arc formed by the data points lies beneath the abscissa, fitting the data points nicely. The equation provides an empirical description of the complex permittivity (ε*).

$$\varepsilon^* = \varepsilon' - \varphi\varepsilon'' = \varepsilon_\infty + \frac{\Delta\varepsilon}{1+(\omega\tau)^\beta} \dots\dots\dots\dots\dots (27)$$

Where, $\Delta\varepsilon=\varepsilon_o-\varepsilon_\infty$,

ε_o is the static permittivity, ε_∞ the permittivity at very high frequencies, τ the angular frequency, τ the mean relaxation time and β the parameter using in the range $0<\beta<1$ to describe the distribution of relaxation time. When β=1, the equation gives semicircle in the plot of ε" vs.ε and is reduced to the non-co-operative single relaxation following the linear Arrhenius relation of the dielectric absorption maximum, f_{max} is expressed as

$$2\pi f_{max}\tau = 1 \dots\dots\dots\dots (28)$$

$$\tau = \frac{1}{2\pi f_{max}} \dots\dots\dots\dots\dots\dots (29)$$

where the symmetry of the absorption and dispersion curves is centred at ^{74}=1. Therefore, fmax can be ascertained using the relaxation time τ that was measured experimentally [108].

3.8. Modulus Spectroscopy:

Many times, the complex modulus M* formalism is employed for dielectric relaxation research. From the impedance data presented by the relation, the real part M′ and the imaginary part MǴ of the complex modulus (M*) can be evaluated.

$$M^* = M' + jM'' = \frac{1}{\varepsilon^*} = j\omega\varepsilon_o Z'' \dots\dots\dots\dots (30)$$

$$where, \quad M' = \frac{\varepsilon'}{(\varepsilon'^2+\varepsilon''^2)} \dots\dots\dots\dots\dots (31)$$

$$M'' = \frac{\varepsilon''}{(\varepsilon'^2+\varepsilon''^2)} \dots\dots\dots\dots\dots (32)$$

One benefit of presenting frequency-dependent dielectric or conductivity data using modulus formalism is that it removes any false effects caused by contacts or surfaces [113, 114]. This type of analysis of the electric data suggests that the electrode polarisation phenomenon adds very little to M* and can be ignored because the real part of the modulus M′ approaches zero at low frequencies. The values of the relaxation time and frequency correlate with the peak in the MǴ fluctuation.
When discussing the synthesis and characterization techniques of nanocomposite polymer electrolyte membranes, several key factors become crucial: scalability, economic feasibility, and repeatability of results. Let us break down each of these aspects in the context of these membranes:

- **Scalability**:

This refers to the ability of the synthesis method to be scaled up from laboratory-scale production to industrial-scale production without significant loss of efficiency or quality. For nanocomposite polymer electrolyte membranes, scalability is essential because these membranes are often intended for practical applications in devices like batteries, fuel cells, and sensors. Techniques that can be easily scaled up, such as solution casting, solvent evaporation, or electrospinning, are typically favored in industrial applications. It is important to ensure that as the production scales, the properties of the membranes remain consistent and desirable.

- **Economic Feasibility:**

The cost-effectiveness of the synthesis and characterization techniques is critical for widespread adoption and commercialization.

Factors influencing economic feasibility include the cost of raw materials, energy consumption during synthesis, labor costs, and equipment costs. Techniques that use readily available, inexpensive materials and involve straightforward processes tend to be more economically feasible. However, cost-effectiveness should be balanced with the performance and longevity of the membranes to ensure competitiveness in the market.

- **Repeatability of Results**:

Consistency in the properties and performance of nanocomposite polymer electrolyte membranes is essential for their reliability and reproducibility. Techniques that yield consistent results across different batches and under varying conditions are preferred. This requires robust characterization techniques that can accurately measure and validate the properties of the membranes, such as mechanical strength, ionic conductivity, thermal stability, and chemical resistance. Quality control measures and standardized protocols play a crucial role in ensuring repeatability.

4. **Potential Areas for Future Research:**

- **Enhanced Performance through Nanoparticle Design**:

Investigating novel nanoparticle designs (e.g., core-shell structures, functionalized surfaces) can improve compatibility with polymer matrices, leading to enhanced mechanical, thermal, and electrochemical properties of membranes.

- **Advanced Characterization Techniques:**

Developing and refining characterization techniques (e.g., in situ imaging, multi-scale modeling) to provide deeper insights into the structure-property relationships of nanocomposite membranes. This can aid in understanding transport mechanisms and optimizing membrane performance.

- **Green and Sustainable Synthesis Methods:**

Exploring environmentally friendly synthesis routes (e.g., green solvents, sustainable nanomaterials) that reduce energy consumption, waste generation, and reliance on hazardous chemicals.

- **Integration with Emerging Technologies:**

Exploring the integration of nanocomposite polymer electrolyte membranes with emerging technologies such as artificial intelligence (AI) for predictive modeling, Internet of Things (IoT) for real-time monitoring, or additive manufacturing (3D printing) for customized membrane fabrication.

- **Application-specific Optimization**:

Tailoring synthesis and characterization techniques to meet the specific requirements of diverse applications (e.g., energy storage, water purification, biomedical devices) to enhance performance under varying conditions.

- **Long-term Stability and Durability:**

Investigating strategies to improve the long-term stability and durability of nanocomposite membranes, including resistance to degradation from chemical exposure, mechanical stress, and aging.

5. Conclusions: Experimental investigations using dielectric spectroscopy, electrical conductivity, XRD, OM, SEM, and IR reveal that nanofiller alters the morphological and physical attributes of the nano-composite electrolyte. The production of a nano-composite system with crystallite sizes ranging from 40 to 60 nm is confirmed by XRD and SEM measurements. When ferrite is dispersed, the electrical conductivity is increased by around 4 orders of magnitude, and it also regulates the gap between crystalline and amorphous conductivity. The amount of salt in the polymer electrolyte affects how well filler fits in. A broad electrochemical window for device applications is demonstrated by the C-V studies. The presence of the material electrode interface polarisation process is

shown by the fluctuation of the relative dielectric constant with frequency (on the lower frequency side) in nano composite electrolytes (NCPEs). It also suggests a strong coupling between segmental mobility of polymers and ions. The dielectric constant's frequency variation is more pronouncedly influenced by the addition of salt than by ferrite. The electrical modulus's scaling behaviour suggests that carrier concentration is also a factor in the relaxing process. As the concentration of salt rises, so does the ac conductivity.

References:

[1]. B. Scrosati., Applications of Electroactive Polymers, Chapman and Hall,London,1993.

[2]. F.M. Gray, Solid Polymer Electrolytes, Fundamentals and Technological Applications, VCH, New York, (1991).

[3]. D. E. Fenton, J.M. Parker, P.V. Wright, Polymer 14 ,1973, 589.

[4]. R. G. Linford, (Ed). Electrochemical Science and Technology of Polymers, 1 and 2, Elsevier Applied Science, London ,1987 and1990.

[5]. N.Srivastava, A. Chandra S.Chandra, Physica. Review, B52 ,1995, 225.

[6]. F. W. Stone, J. J Stratta., "Ethylene Oxide Polymers" In Encyclopedia of Polymer Science and Technology, Vol. 6, John Wiley &Sons, Inc New York, 1967, 103.

[7]. L. Yang, G. Venkatesh, R. Fassihi, "Characterization of compressibility and Compactibility of Poly (ethylene oxide) Polymers for Modified Release application by Compaction Simulator," J. Pharm. Sci. 85, 1996,1085.

[8]. P.G., Bruce, F. Grey, D. F Shriver, in Solid State Electrochemistry, Bruce. G. Ed. Cambridge University Press: Cambridge, U. K. ,1995.

[9]. W. Wieczorek, D. Raducha, A. Zaiewska, J. R. Stevens, J. Phys. Chem. 1998.

[10]. D. B. Braun., "Poly (ethylene oxide)" in Handbook of Water-Soluble Gums Resins, R. L. Davidson, Ed. (McGraw – Hill Book Company, New York, 1980 19

[11]. N. B. Graham, "Hydrogels for Useful Therapy," special publication, Royal Society of Chemistry, 87(High Value Polymers), 1991, 79.

[12]. N.B. Graham et al., "Caffeine Release from Fully Swollen Poly (ethyleneoxide) Hydrogels," J. Controlled Release 5, 1988, 243.

[13]. M.F. Daniel, B. Desbat, J.C. Lassegues, Solid State Ionics28, 1988 632.

[14]. A. Awadhia, S. L.Agrawal Solid State Ionics, 178, 2007, 951.

[15]. B. Brunetand, J. Cabane. Non-Cryst. Solids163, 1993, 211.

[16]. N. Chand, N. Rai, T. S. N. Natarajan S.L. Agrawal Fibres and Polymers, 12 2011, 438.

[17]. B.K. Choi, K.H. Shin, Solid State Ionics, 86, 1996, 303.

[18]. W. Wieczorek, J.R. Stevens, Z. Florzanczyc, Solid State Ionics, 85, 1996, 67.

[19]. D. Golodnisky, G.Ardel, E.Peled, Solid State Ionics, 85, 1996, 231.

[20]. Bhide, K. Hariharan, Polymer International, 57, 2008, 523.

[21]. S. S. Sekhon, G.S. Sandha, S.Chandra, Bull. Electrochem. 12, 1996, 415.

[22]. A. Chandra, P.K.Singh, S.Chandra, Solid State Ionics 15, 2002, 154.

[23]. D.K. Pradhan, R. N.P. Choudhary, B.K. Samantaray Express Polymer Letters 2,2008, 630.

[24]. F. Croce, L.Persi, F.Ronci, B.Scrosati, Solid State Ionics, 135, 2000, 47.

[25]. S. Chung, Y.Wang, L.Persi, F.Croce, S. G. Greenbaum, B. Scrosati, E. Plichta, J. Power Sources 97, 2001, 644.

[26]. M. Abdullah, W. Lenggoro, K. Okuyama, Encyclopedia of nanoscience and nanotechnology Edt. H.S. Nalwa, 8, 2004, 731.

[27]. M. Popovici, C. Savii, D. Niznanskya, J. Subrta, J. Bohaceka, D. Becherescub, C. Caizerc, C. Enache, C. Ionescu Journal of Optoelectronics and Advanced Materials, 5, 2003, 251.

[28]. K. Pandey, M.M. Dwivedi, M. Singh, S. L Agrawal., J. Polym. Res.17, 2010, 127.
[29]. B. Jirgensons, M.E. Straumanis, A Short Text Book of Colloid Chemistry, Pergamon Press, Oxford 1962,377.
[30]. S. Chandra, S. S. Sekhon, R. Shrivastava, N. Arora, Solid State Ionics,154, 2002, 609.
[31]. Tager, Physical Chemistry of Polymer, MIR Publisher, Moscow,1978.
[32]. M. S. Siekierski, Ph.D. Thesis, Warsaw Univ. of Tech., Warsaw, 1994.
[33]. S. Rabaste, Microcavitésoptiqueélaboréesparvoie sol-gel: applications aux ions terre rare d, Eu3+ et aux nanocristauxsemiconducteurs de CdSe, PhD thesis, Lyon, 1993.
[34]. B. Fabes et al 'Sol-Gel Derived Ceramic Coatings' in Ceramic Coatings and Films, ed. by J.B. Wachtman and R.A., Haber Noyes Publications, New Jersey, 1993.
[35]. M. Kakihana Journal of Sol-Gel Science and Technology, 6,1996, 7.
[36]. L.L. Hench, J. K. West, Chemical Review, 90, 1990, 33
[37]. Y. Narendar, G.L Messing, Catalysis Today, 35,1997, 247.
[38]. V. Driessche, B.Schoofs, G. Penneman, E. Bruneel, S.Hoste Measurent Science Rev., 5, 2005, 3.
[39]. C.J. Brinker, G.W. Scherer Sol-Gel Science, The Physics and Chemistry of Sol-Gel Processing, Academic Press, Boston, 1990.
[40]. B. Arkles, Kirk-Othmer Encyclopedia of Chemical Technology, John Wiley, New York,1997, 69.
[41]. A. C. Pierre, Introduction to sol-gel processing. Springer Nature, 2020
[42]. C. J. Brinker & G. W. Scherer, Sol-gel science: the physics and chemistry of sol-gel processing. Academic press. 2013
[43]. Y. Lu, H. Fan, N. Doke, D. A.Loy, , R. A. Assink, , D. A. LaVan, & C. J. Brinker, Evaporation-induced self-assembly of hybrid bridged silsesquioxane film and particulate mesophases with integral organic functionality. Journal of the American Chemical Society, 122(22), 2000 5258-5261.
[44]. K. Gopinath, S.Gnanasekar, , K. A. Al-Ghanim, M.Nicoletti, M.Govindarajan, A. Arumugam & S. Thanakkasaranee, Fabrication of neodymium (Nd), cadmium (Cd) and Nd: Cd doped hybrid copper oxide nanocomposites: evaluation of their antibacterial activity and cytotoxicity against human L132 cell line. Ceramics International, 49(18), 2023, 29933-29947.
[45]. M. S. Hassan, One pot synthesis of CoTiO3-TiO2 composite nanofibers and its application in dye degradation. International Journal of Chemoinformatics and Chemical Engineering (IJCCE), 8(2), 2019.47-56
[46]. Z.L. Lu, E. Lindner, H. A Mayer., Chem. Rev. 102, 2002, 3543.
[47]. A.C. Pierre, Introduction to Sol-Gel Processing. Kluwer, Boston, 1998.
[48]. B.D. Cullity, Elements of X-ray diffraction, Addison Wesley, Co.USA 1978.
[49]. J. Bonarski, "X-ray texture tomography of near-surface areas" Progr. Mat. Sc. 51, 2006, 61.
[50]. John Wiley & Sons Ltd. Elements of Modern X-Ray Physics, 2001, 40
[51]. B.E Warren, X-ray Diffraction, General Publishing Company, Classic X-Ray physics book ,1990.
[52]. Charles Hodgeman, Ed. CRC Handbook of Chemistry, and Physics, 44thEd. USA: Chemical Rubber Co. 1961.
[53]. W.L. Bragg, "The Diffraction of Short Electromagnetic Waves by a Crystal", Proceedings of the Cambridge Philosophical Society, 17, 1913, 43–57.
[54]. M. Taubin, V Platonov, A. Yaskolko X-Ray Tube Cathodes of Medical Purpose. Biomed Eng.;43(1) 2009, 48-50.
[55]. G. K. Williamson, W.H. Hall, X-ray line broadening from filed Aluminium and wolfram, Acta Metall. 1 ,1953, 22.
[56]. P. Habdas, E.R Weeks., Curr. Opinion in Coll. &Interf. Sci. 2002

[57]. D. Semwogerere, E.R. Weeks Confocal Microscopy, in Encyclopedia of Biomaterials & Biomedical Engineering, Taylor&Francis, 2005**.**

[58]. J.T. Rantala, P. Ayras, R. Levy, S. Honkanen, M.R. Descour N. Neogrammarian,"Binary phase zone-plate arrays based on hybrid sol-gel glass," Opt. Lett., 23, 1998, 1939.

[59]. Max. Knoll, "Aufladepotentiel and SekundäremissionElectronEnbestrahlter Korper", ZeitschriftfurtechnischePhysik, **16 ,1935,** 467.

[60]. J. Goldstein, Scanning electron microscopy and x-ray Microanalysis, Kluwer Academic/Plenum Publishers, 2003, 689.

[61]. L. Reimer, Scanning electron microscopy: physics of image formation and Microanalysis, Springer, 1998, 527.

[62]. R. F. Egerton, Physical principles of electron microscopy, an Introduction TEM, SEM, and AEM, Springer, 2005, 202.

[63]. R. Clarke, Microscopy techniques for materials science, CRC, 2002.

[64]. P. R. Griffiths and J.A. Haseth de, "Fourier Transform Infrared Spectroscopy," John Wildey& Sons, New York, 1986.

[65]. L. Smith, Applied Infrared Spectroscopy, New York: Wiley,1979.

[66]. R. M. Crooks et.al, "The Characterization of Organic Monolayers by FTIR External Reflectance Spectroscopy," Spectroscopy 7, 1993, 28.

[67]. C. Daniel Harris, and D. Bertolucci. Michael Symmetry and Spectroscopy: An Introduction to Vibrational and Electronic Spectroscopy. New York: Dover Publications, 1989. Print.

[68]. S. C. Lassegues, Desbat B., O. Tringquet, F. Cruege, Solid State Ionics, 35 ,1989, 17.

[69]. Sharma B. K., Instrumental Methods of Chemical Analysis, Goel Publishing House, Meerut (7thedn), 1998.

[70]. K. Nakamoto, Infrared and Raman Spectra of Inorganic and Coordination Compounds(4thedn), John Wiley & sons, New York, 1988.

[71]. M. I Pope, M.J. Judd, "Differential Thermal Analysis", London, Heyden, Academic Press 1977.

[72]. J. Sestak, V. Satava, W.W. Wendland Thermochimica Acta,7, 1973,333.

[73]. Konryushin & L.N. Larikov: J. Mat. Sci., 13, 1978,1.

[74]. L. Greer, ThermochimicaActa, 42,1980,193.

[75]. S. Etemad, A.J. Heeger, & A.G. Mac Diarmid, Annu. Rev. Phys. Chem.33, 1982,443.

[76]. P.K. Shukla, Study of Polymer Electrolytes for Electrochromic Display Devices, Ph. D. Thesis, A. P. S. University, Rewa, 1997.

[77]. P.T. Kissinger, W.R. Heineman, J. Chem. Educ.60, 1983, 702.

[78]. H. Karami, B. Kafi, S. N Mortazavi, Int. J. Electrochem. Sci.,4,2009,414.

[79]. W. W. Yao, H.M. Peng, R. D Webster, M. W Gill Peter, J. Phys.Chem. B, 112 2008, 6847.

[80]. J. S. Wagner, C. Wagner, J. Chem. Phys., 26, 1957, 1597.

[81]. A. R. Kulkarni, S. Selvasekarapandian, K. Hariharan, S. A. Suthanthiraraj, S. Selladurai, B. Nalini, Vijay Kumar, and M. (eds.) Proc. National Workshop on Solid State Ionics and Its Applications, Bharathiar University, Coimbatore 2002.

[82]. J. Przyluski, W. Wieczorek, Mat. Sci. and Engg. B13 ,1992,335.

[83]. A. A. Khamzin, I. I. Popov, And R. R. Nigmatullin, Correction of The Power Law of Ac Conductivity in Ion-Conducting Materials Due to The Electrode Polarization Effect Physical Review E 89, 2014, 032303

[84]. Rubintein (Ed.), Physical Electrochemistry: Principles, Methods and Applications, Marcell Dekker, New York ,1995.

[85]. D. W. Xia, J. Smid, Recent Advances in Fast Ion Conducting Materials and Devices, B. V. R. Chowdari, Q.Liu and

L. Chen (eds), World Scientific, Singapore,1990, 249.
[86]. J. E. Baurale, J. Phy. Chem. Solids, 30 1969, 2657.
[87]. S. Slane, M. Saloman, J. Power Sources, 55, 1995, 7.
[88]. B. E. Mallander, A. Luden, Materials for Solid State Batteries, (Eds.) B. V. R. Chowdari and S. Radhakrishna, World Scientific, Singapore, 1986, 161.
[89]. W. I. Archen R. D. Armstrong, in: Electrochemistry, vol. 7 (Ed.), H. R. Thirsk the Royal Soc. of Chem., London, 1980, 157.
[90]. K. S. Cole, R. H. Cole J. Phys., 9, 1941, 341.
[91]. S. P. S. Badwal, Solid State Batteries, B. V. R. Chowdari, S. Radhakrishna, World Scientific, Singapore, 1988, 965.
[92]. Wood J., Materials Today, 10, 2005, 16.
[93]. K. Johnscher, J. M. Reau, Mat. Sci. 13 1978, 563.
[94]. G. Williams, D. C. Watts and in Dielectric Properties of Polymer, (Ed.) F. E. Karazz, Plenum Press, New York 1972, 17.
[95]. S. L. Agrawal, P. K Shukla, Phy. Stat. Sol.163, 1997, 247.
[96]. P. Muistarelli, A. Magistris, P. Ferloni, Mol. Cryst. Liq. Crystal,229, 1993,187.
[97]. H. Shirkawa, E.J. Louis., A.G. Mac Diarmid , Chiang C.K. Heeger, A.J., J. Chem.Soc. Chem. Commun., 1977,578.
[98]. S. Etemad, A.J. Heeger, A.G., MacDiarmid, Annu. Rev. Phys. chem. 33,1982, 443
[99]. J. R. Macdonald (Ed.), Impedance Spectroscopy – Emphasizing Solid Materials and System, John Wiley & Sons, New York ,1987.
[100]. M.C. Wintersgill, Fontanalla, in Polymer Electrolyte Review-II, MacCallum J.R. and Vincent CA (eds.), Elsevier, London ,1987.
[101]. H. Eliasson, I. Albinsson B.E. Mellander, Electrochemica Acta 43 1998, 1498.
[102]. K.P. Singh, P. N. Gupta European Polymer Journal, 34, 1998, 1023.
[103]. B. Natesan, N.K. Karan et al J. Non Crystalline Solids352, 2006,5205.
[104]. D. K. Pradhan, R.P.N Choudhary, J. Power Sources139, 2005, 384.
[105]. T. J. Pinnavaia, G. W. Bell (eds.) Polymer-Clay Nanocomposite, JohnWiley and Sons Ltd. England 2000,1.
[106]. M.Wang, F Zhao, Z. Guo, and S. Dong, Electrochemica Acta, 49, 2004, 3595.
[107]. K. Jonscher, Dielectric relaxation in Solids, Chelsea Dielctric Press, London, 1983.
[108]. K. Jonscher, Nature, 267,1977, 673.
[109]. K. A. Mauritz Macromolecules, 22, 1989, 4483
[110]. S.R. Elliott Solid State Ionics, 27 ,1988, 131.
[111]. M.L. Lucia Leon, and J. Santamaria, Phys. Rev. B 55, 1997, 882
[112]. D.K. Pradhan, R.N.P Choudhary, B.K. Samantaray Int. J. Electrochem.Sci.3,2008, 597.
[113]. H. A. Hashen and S. Aboulhassan Chinese Journal of Physics 43, 2005, 955.